



Glass and glass ceramic for nonlinear optics: fundamentals to applications

T. Cardinal, E. Fargin, J. J. Videau, Y. Petit, G. Guery (*ICMCB*)

M. Dussauze, F. Adamietz, V. Rodriguez (*ISM*)

L. Canioni, A. Royon (*LOMA*)



NonLinear Optical Materials

Nonlinear Parameters

Third order Nonlinearities

Second order Nonlinearities

Nonlinear Absorption

□ Nonlinear optical effects

$$\mathbf{P} = \epsilon_0 \left(\chi^{(1)} \mathbf{E}(\omega) + \chi^{(2)} \mathbf{E}(\omega) \mathbf{E}(\omega) + \chi^{(3)} \mathbf{E}(\omega) \mathbf{E}(\omega) \mathbf{E}(\omega) + \dots \right)$$

$\chi^{(1)}$ → n_0
SHG (2ω)
THG (3ω)

$n \approx f(E)$
 $n \approx f(E^2)$

$n = n_0 + \zeta E$
 $n = n_0 + n_2 I$

P : Polarisation
 E : Electric Field
 $\chi^{(n)}$: Linear and Nonlinear susceptibilities

n : Refractive Index
 SHG : Second Harmonic Generation
 THG : Third Harmonic Generation

Third order nonlinearity

- Four wave mixing

$$\chi^{(3)}(-\omega_4, \omega_1, -\omega_2, \omega_3)$$

- Kerr effect

$$\chi^{(3)}(-\omega, \omega, -\omega, \omega)$$

Self focusing
Self phase modulation
Soliton Propagation
Optical switching

- Third Harmonic generation

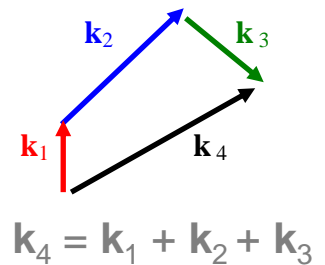
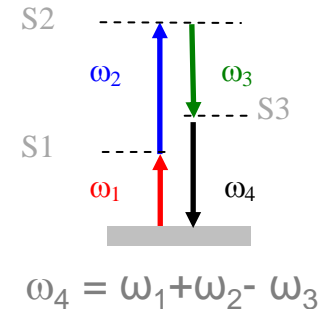
$$\chi^{(3)}(-3\omega, -\omega, \omega, \omega)$$

- Stimulated Raman

$$\chi^{(3)}(-\omega_s, \omega_p, -\omega_s, \omega_p)$$

- Two photon absorption

$$\chi^{(3)}(-\omega, -\omega, \omega, \omega)$$



The formalism of nonlinear optics

- **Polarization of the material** described by a perturbative development:

$$\vec{P}_i(\vec{r};t) = \underbrace{\cancel{\vec{P}_i^{(0)}(\vec{r};t)} + \vec{P}_i^{(1)}(\vec{r};t)}_{\text{linear polarization}} + \underbrace{\cancel{\vec{P}_i^{(2)}(\vec{r};t)} + \vec{P}_i^{(3)}(\vec{r};t) + \dots}_{\text{nonlinear polarization}}$$

- **3rd-order polarization:**

$$\vec{P}_i^{(3)}(\vec{r};t) = \varepsilon_0 \int_{-\infty}^t \int_{-\infty}^t \int_{-\infty}^t R_{ijkl}^{(3)}(\vec{r};t-t_1, t-t_2, t-t_3) \vec{E}_j(\vec{r};t_1) \vec{E}_k(\vec{r};t_2) \vec{E}_l(\vec{r};t_3) dt_1 dt_2 dt_3$$

- **3rd-order susceptibility** = Fourier transform of the 3rd-order response function. → describes the nonlinearities of the glass.

$$\chi_{ijkl}^{(3)}(-\omega_\sigma; \omega_1, \omega_2, \omega_3) = \int_{-\infty}^{+\infty} R_{ijkl}^{(3)}(t_1, t_2, t_3) \exp[i(\omega_1 t_1 + \omega_2 t_2 + \omega_3 t_3)] dt_1 dt_2 dt_3$$

The different contributions to the nonlinear response

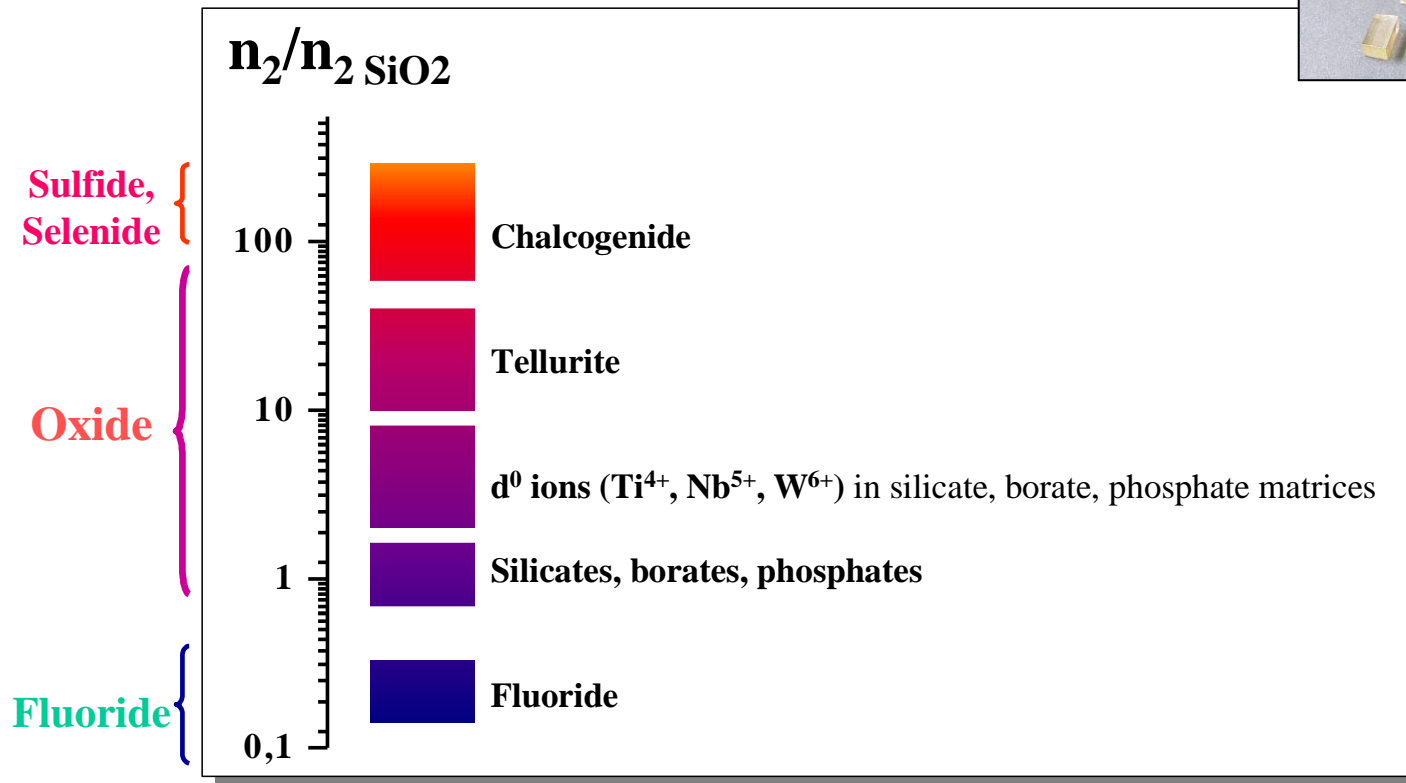
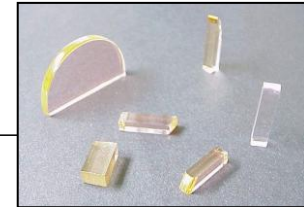
- **Electronic polarization:** instantaneous nonlinear distortion of the electronic cloud around the nucleus (response time ~ 1 fs).
- **Nuclear response:** rearrangement of the nucleus position in the new potential created by the electrons electric field (response time ~ 100 fs-1 ps).
- **Electrostrictive response:** increase of the density, inducing an increase of the nonlinear response (response time ~ 1 ns).
- **Thermal response:** absorption of the electric field followed by dissipation of the energy under the form of heat, inducing a variation of the nonlinear response (response time ~ 10 μ s).

$$\chi^{(3)} = \chi_{elec}^{(3)} + \chi_{nuc}^{(3)} + \cancel{\chi_{str}^{(3)}} + \cancel{\chi_{th}^{(3)}}$$

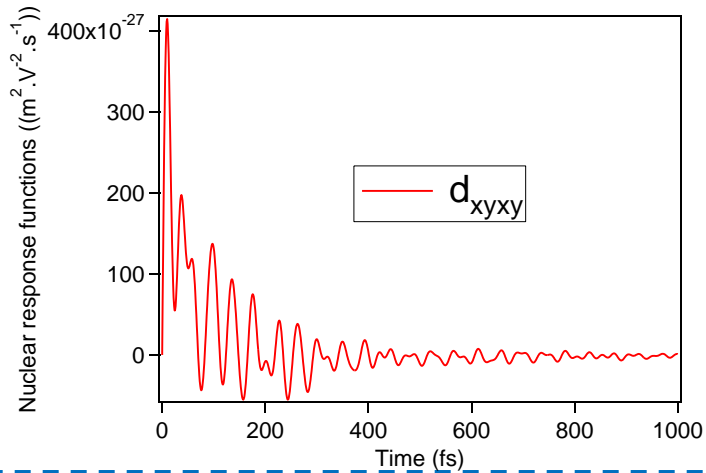
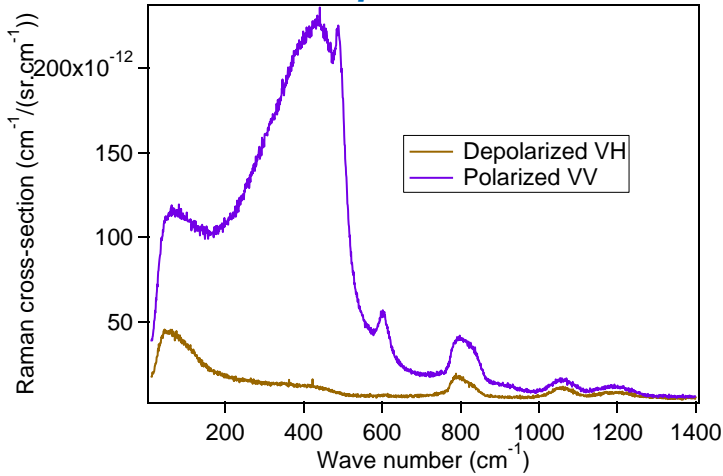
With fs pulses, electrostrictive and thermal contributions are neglected because their building-up time is too long compared to the pulse duration.

Third order nonlinearity

Measured at 1.5 μm

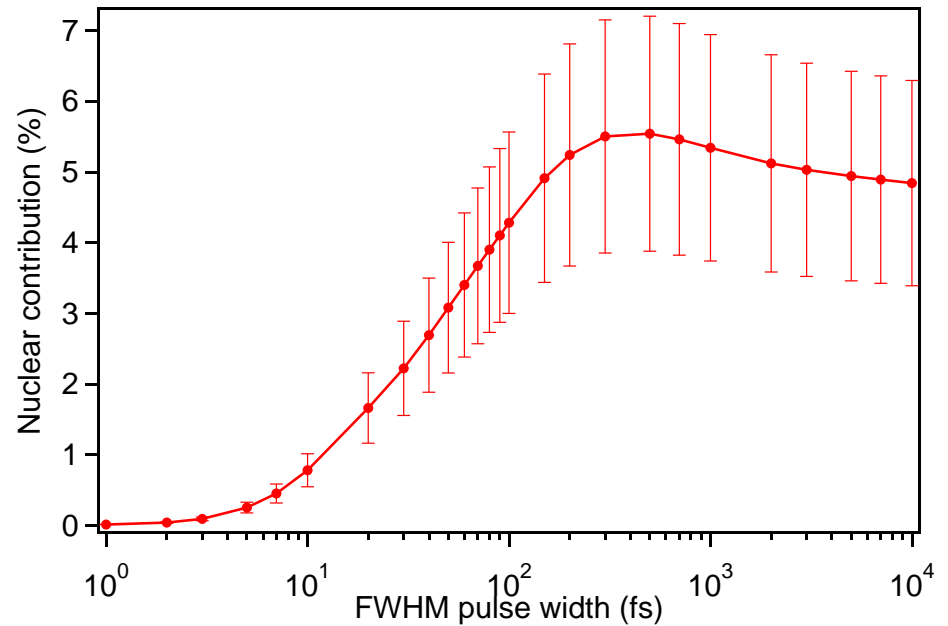


Raman Spectrum



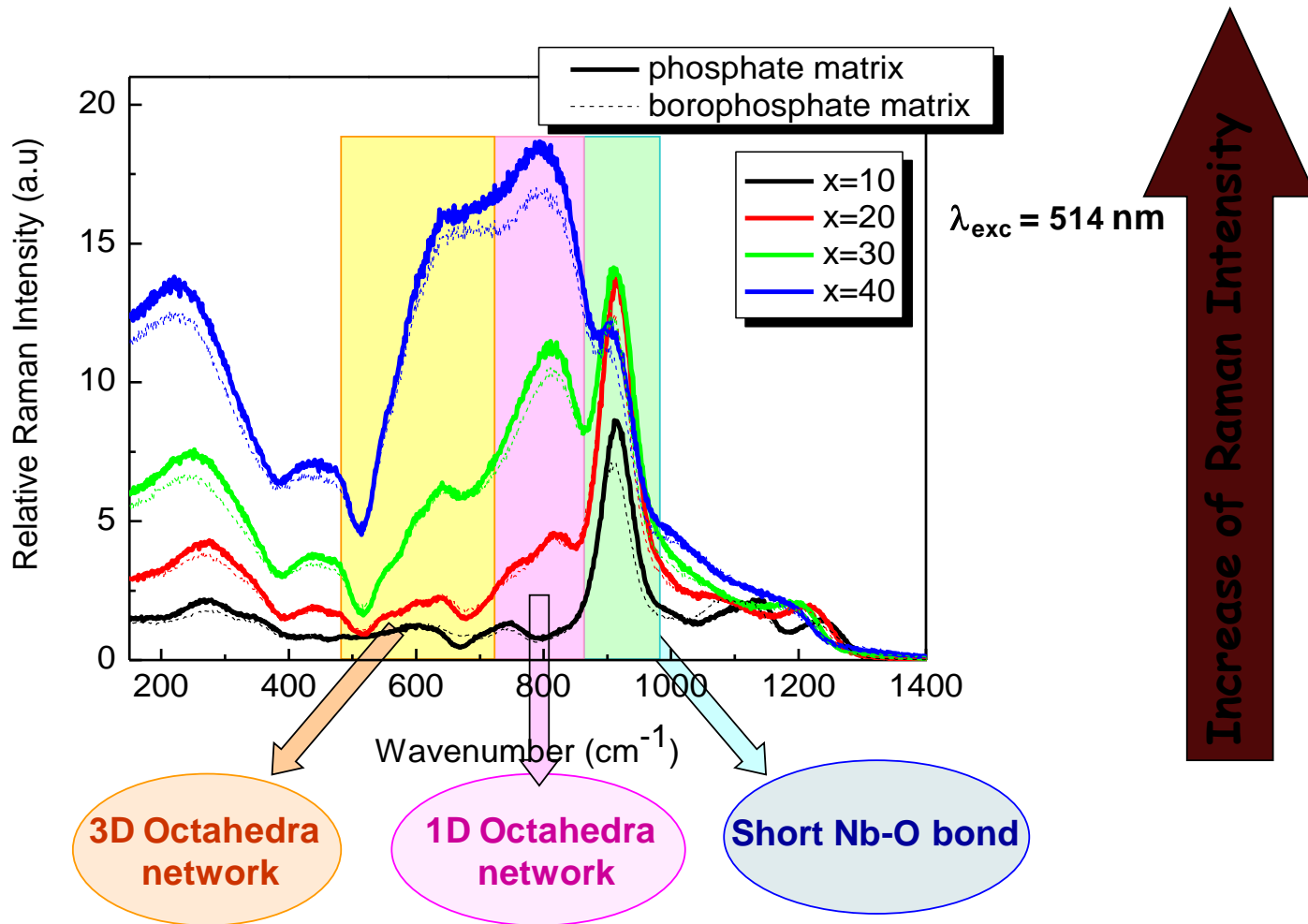
Vibrational Contribution

$$\sigma_{xxxx}^{(3)} = 2.65 \times 10^{-22} \text{ m}^2 \cdot \text{V}^{-2}$$



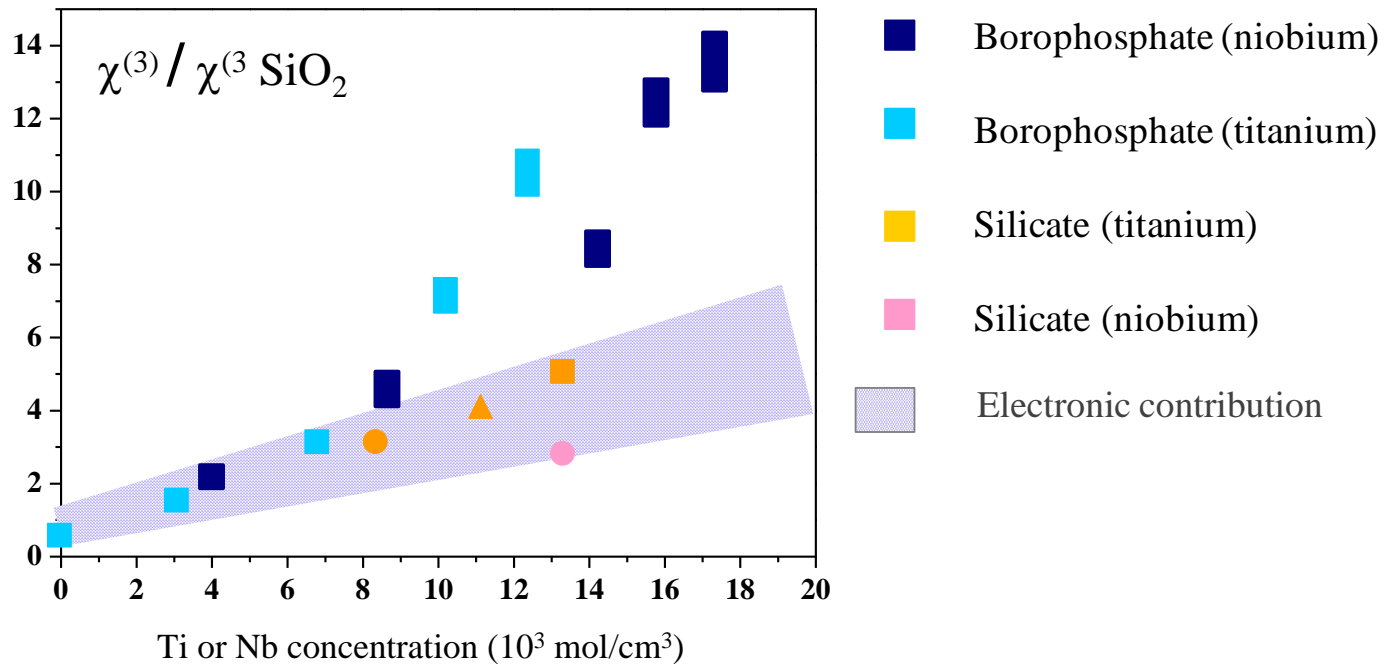
Nuclear contribution up to 6% to the n_2

Niobium oxide containing Glasses

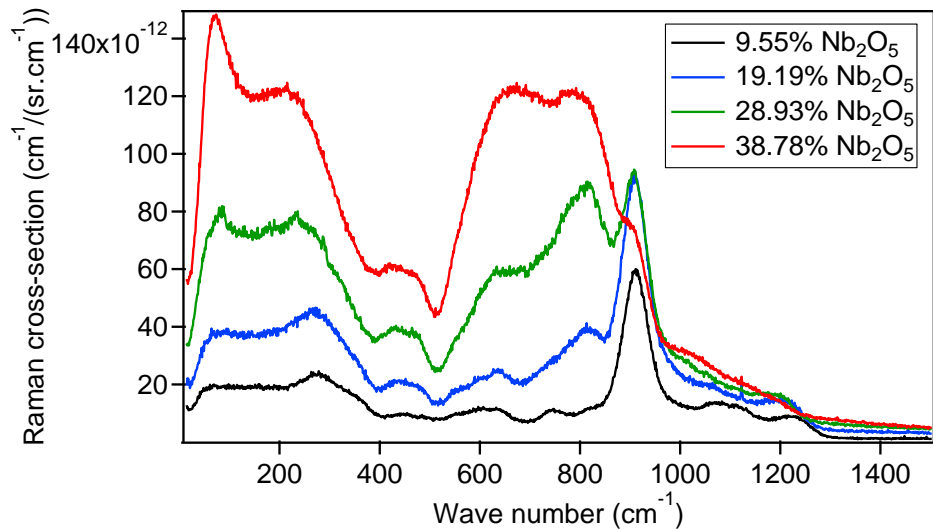
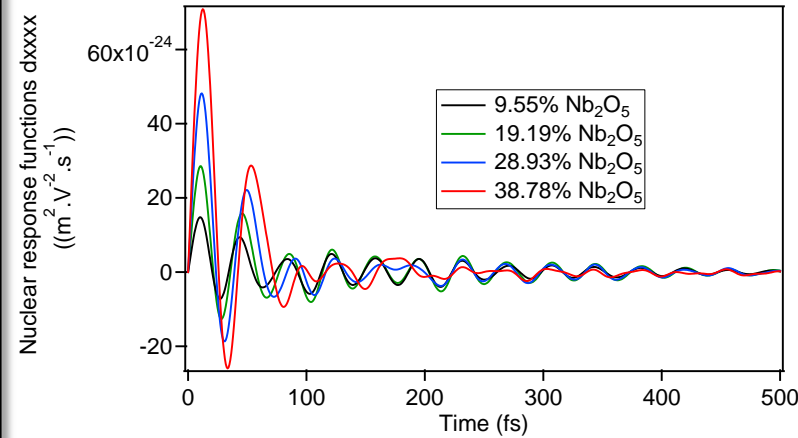
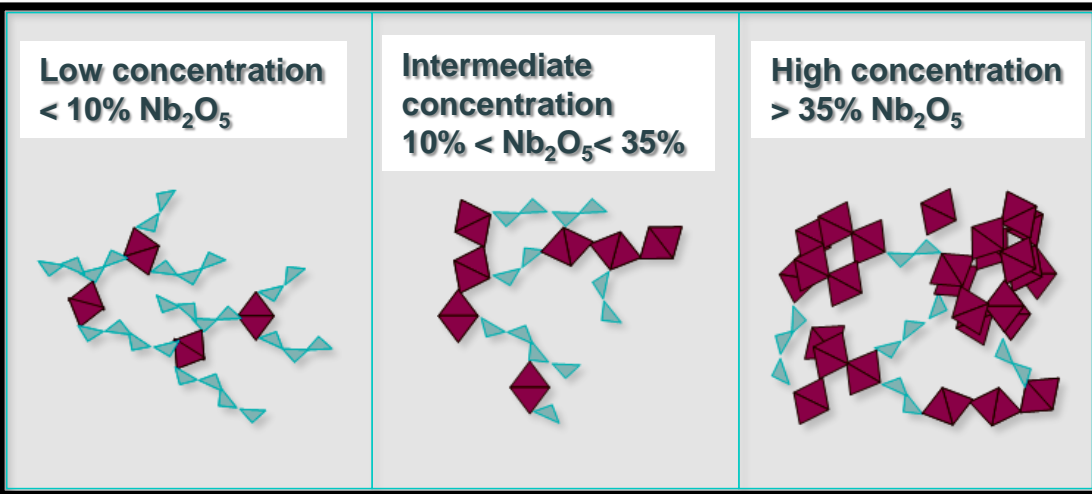


Evolution of the Kerr effect

Measured at 800 nm



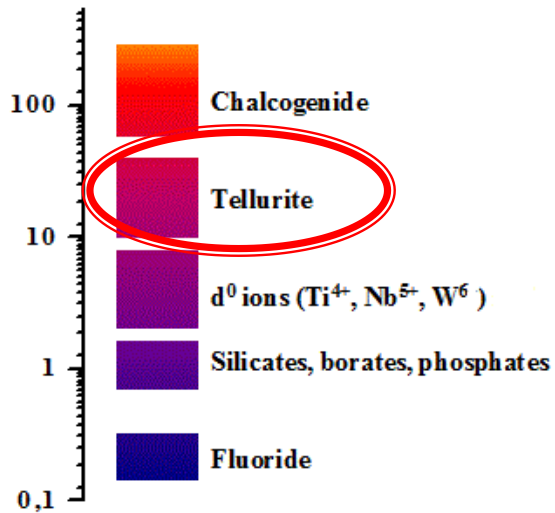
Glass local structure



From less than **10%**
of **nuclear contribution**
to **60%**
to the **n₂**

Structural units of Tellurite network

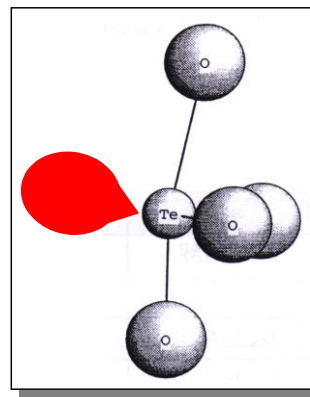
$n_2/n_2 \text{ SiO}_2$



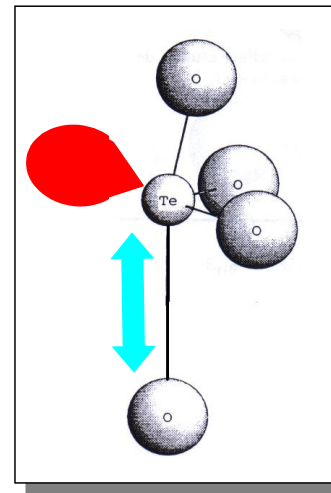
TeO_2

$\text{TeO}_2 + 15\% \text{Al}_2\text{O}_3$

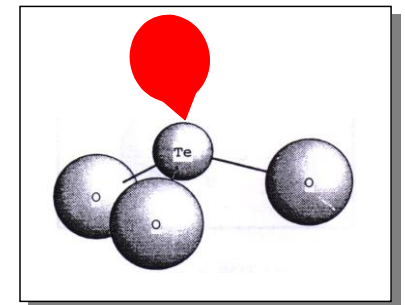
TeO_4 unit



TeO_{3+1} unit



TeO_3 unit

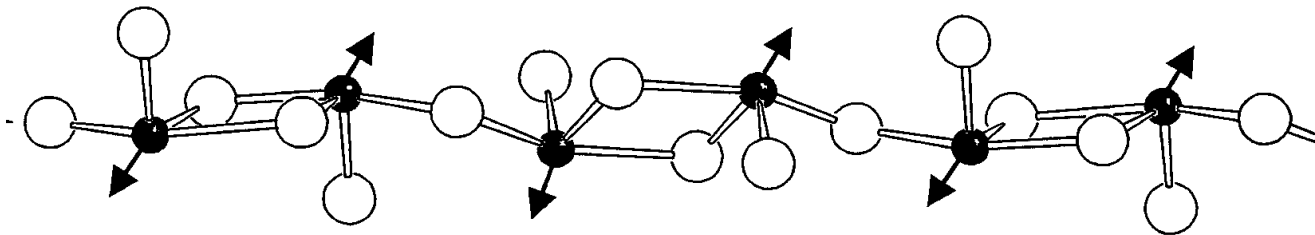


Decrease of polarisability and hyperpolarisability

Medium range order

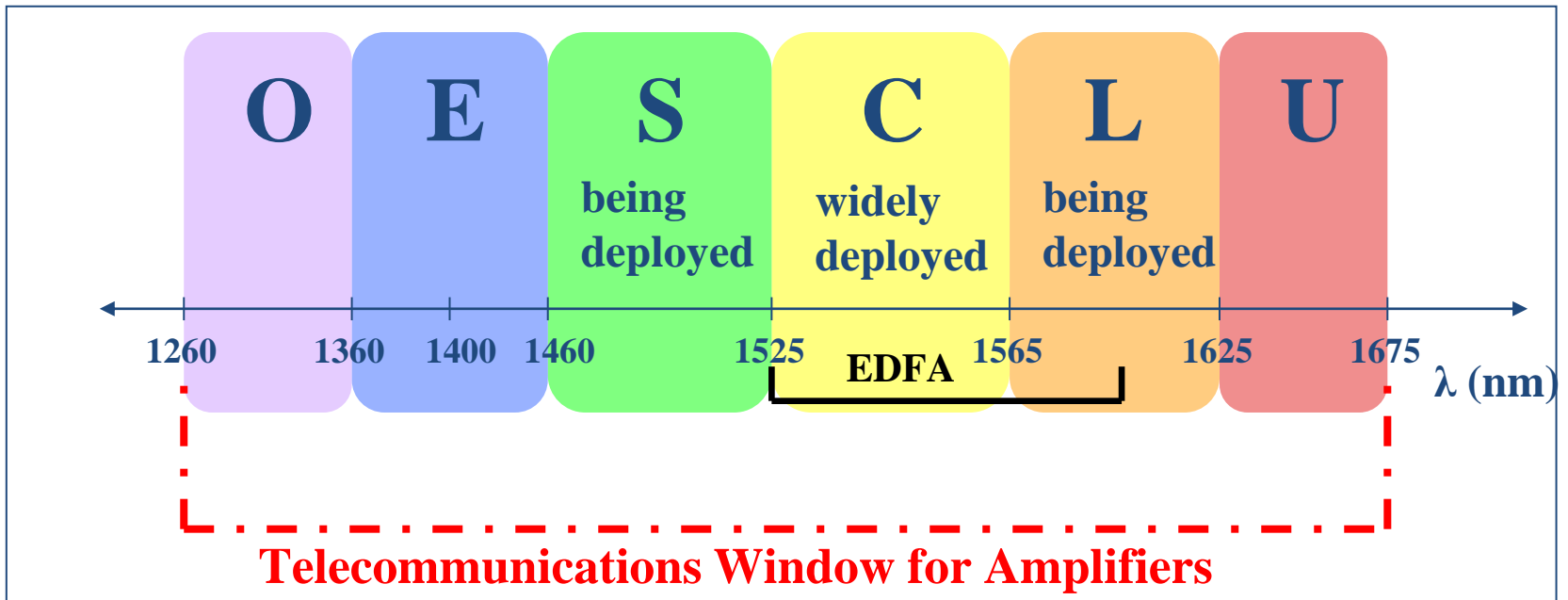
OKE : optical Kerr effect

Tellurium-Thallium glass	50TeO ₂ -50Tl ₂ O	70TeO ₂ -30Tl ₂ O Electronic	75TeO ₂ -25Tl ₂ O
THG susceptibility ($\times 10^{-22} \text{ m}^2 \cdot \text{V}^{-2}$) ($\pm 30\%$)	1042.1	973.4	668.9
OKE susceptibility ($\times 10^{-22} \text{ m}^2 \cdot \text{V}^{-2}$) ($\pm 10\%$)	29.4	47.6	48.2



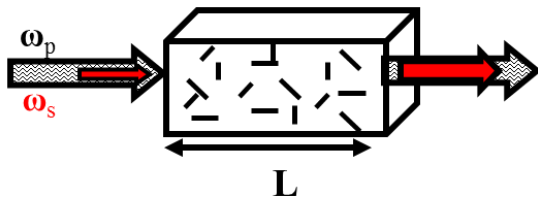
Strong relation between the **glass network** and the **third order nonlinearity**

Fiber Transmission

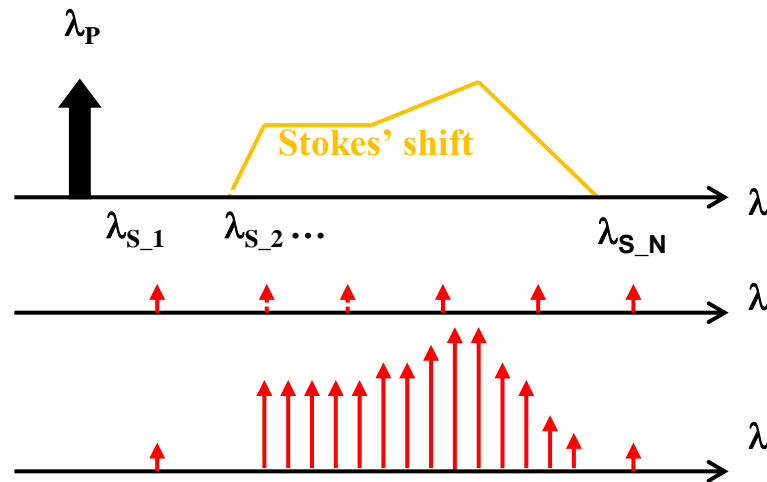
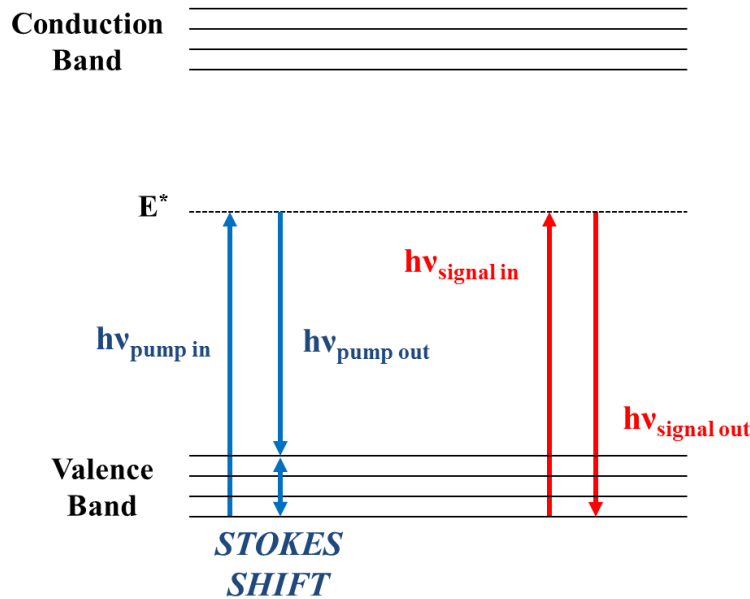


Raman gain

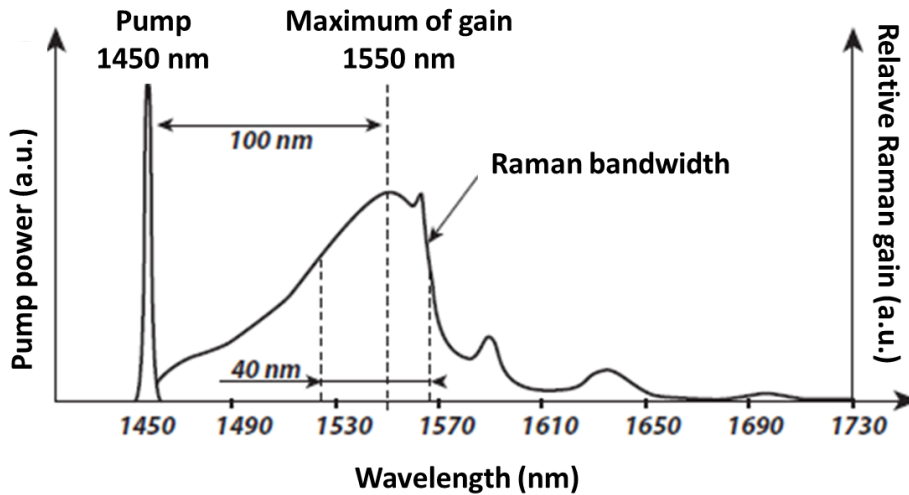
$$P_i = \epsilon_0 \left(\chi_{ij}^{(1)} E_j + \chi_{ijk}^{(2)} E_j E_k + \chi_{ijkl}^{(3)} E_j E_k E_l + \dots \right)$$



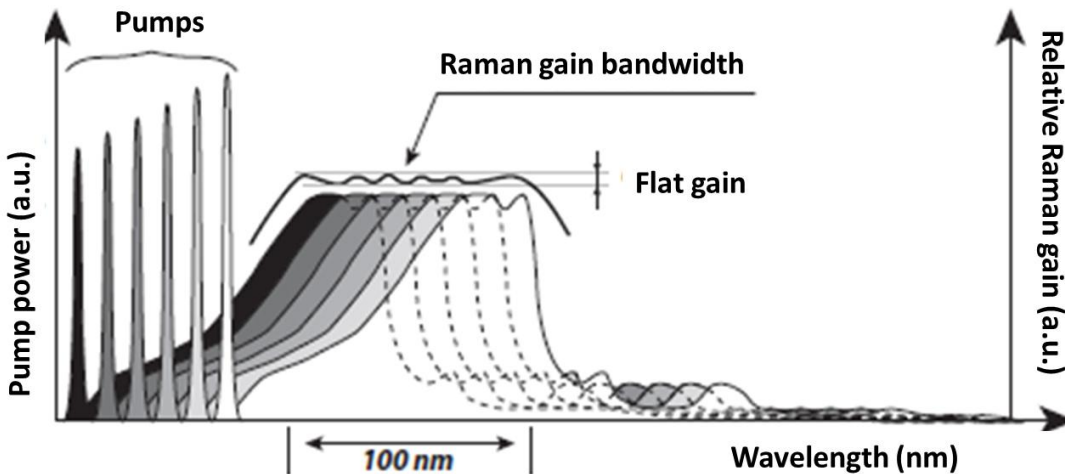
Raman gain results from 4 waves mixing phenomena (3rd order nonlinearity) combining excitation, signal and vibration mode.



Raman gain in fused silica

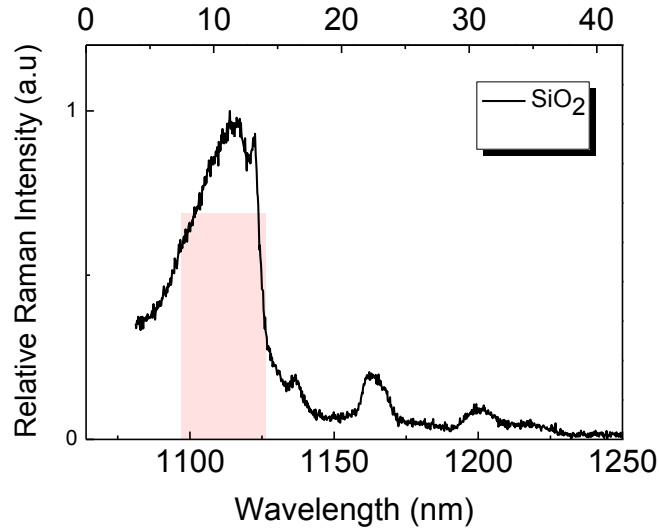


Raman gain bandwidths are fixed by the **bandwidth of the Raman active medium.**

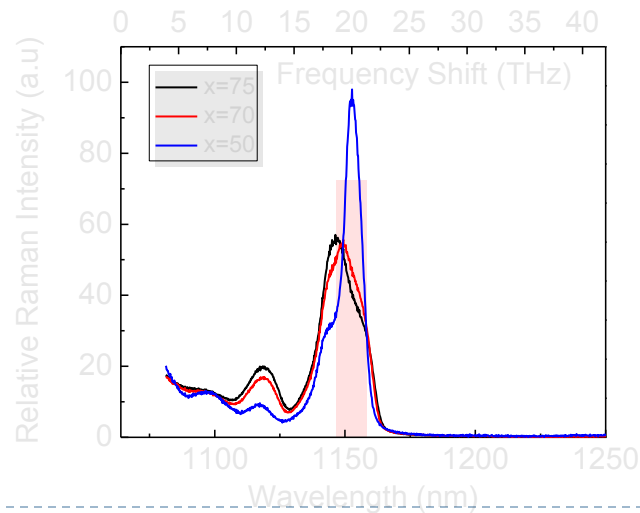
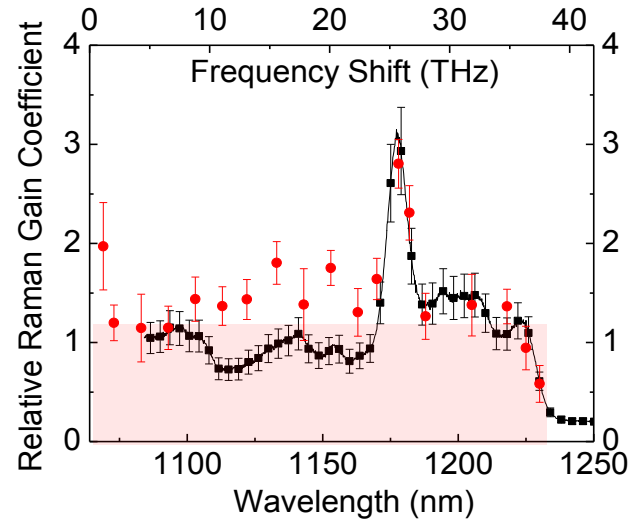


Raman Gain Spectrum

SiO_2

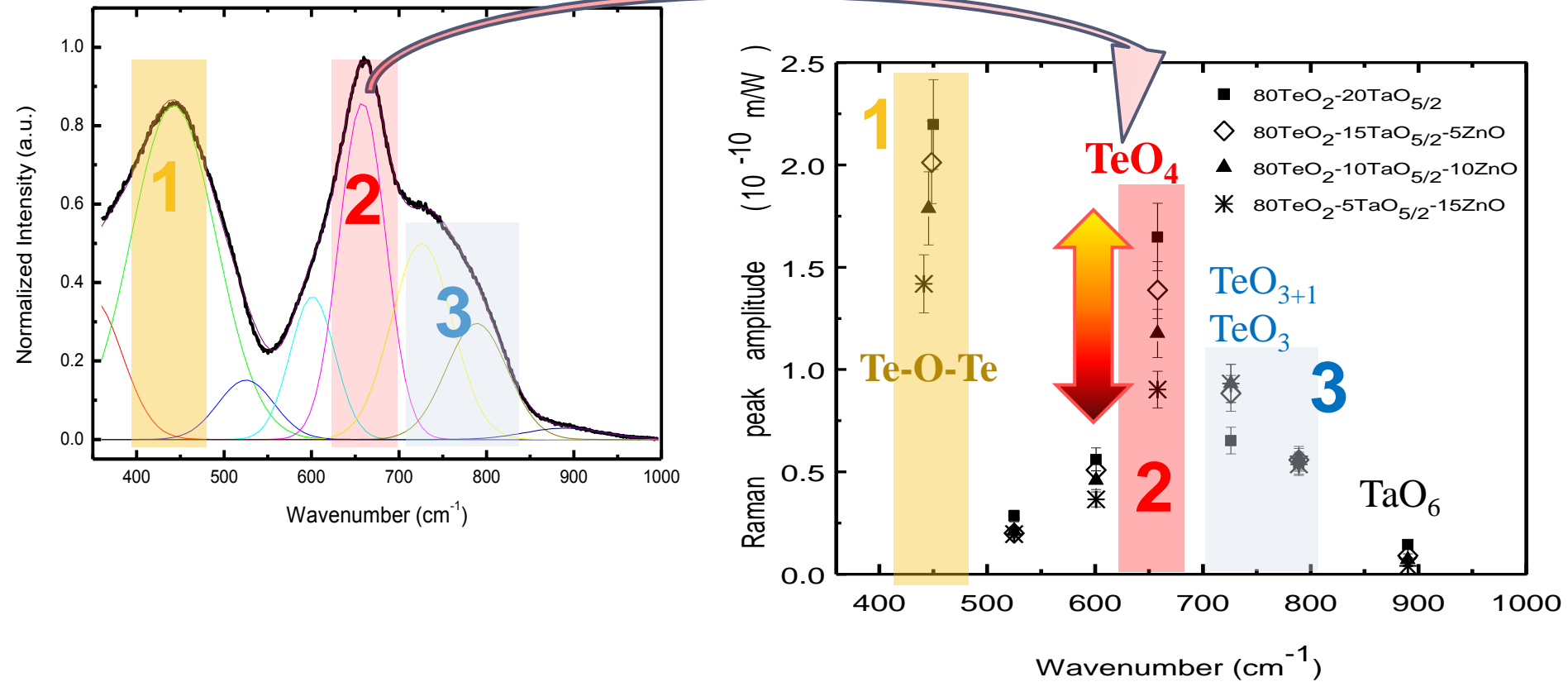


Borophosphate



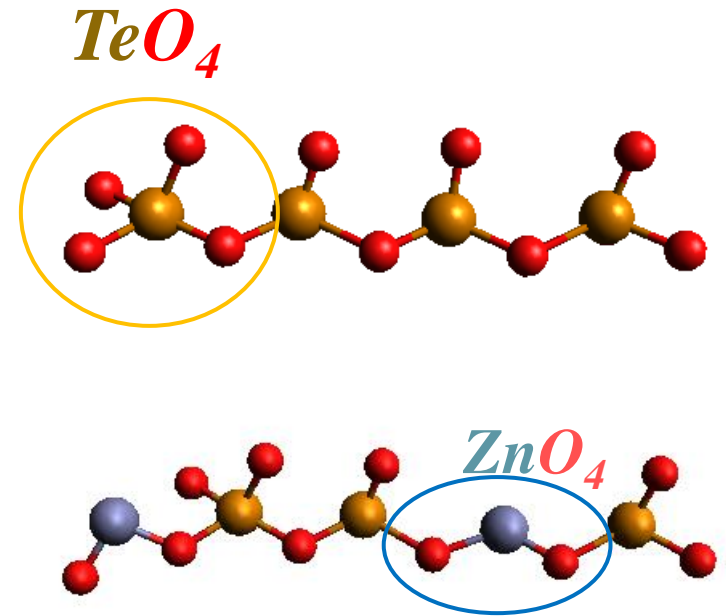
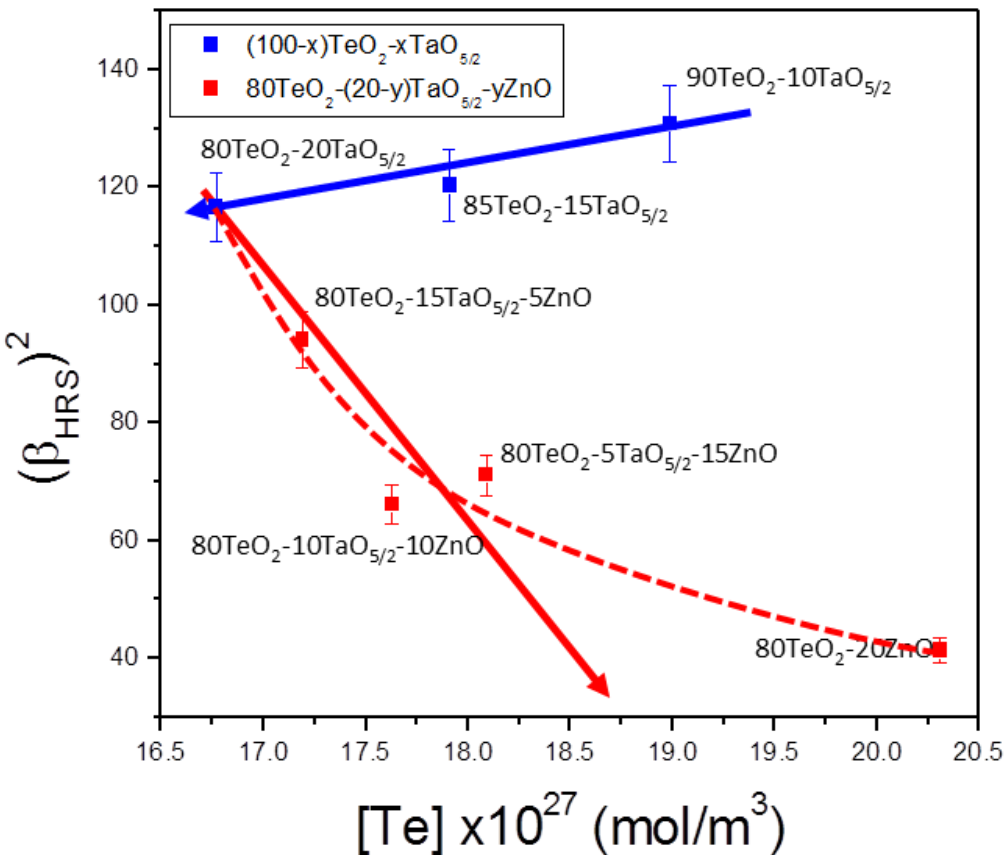
$x \text{ TeO}_2 - (100-x) \text{ TiO}_{0.5}$

Vibrational response



Hyperpolarisability and glass structure

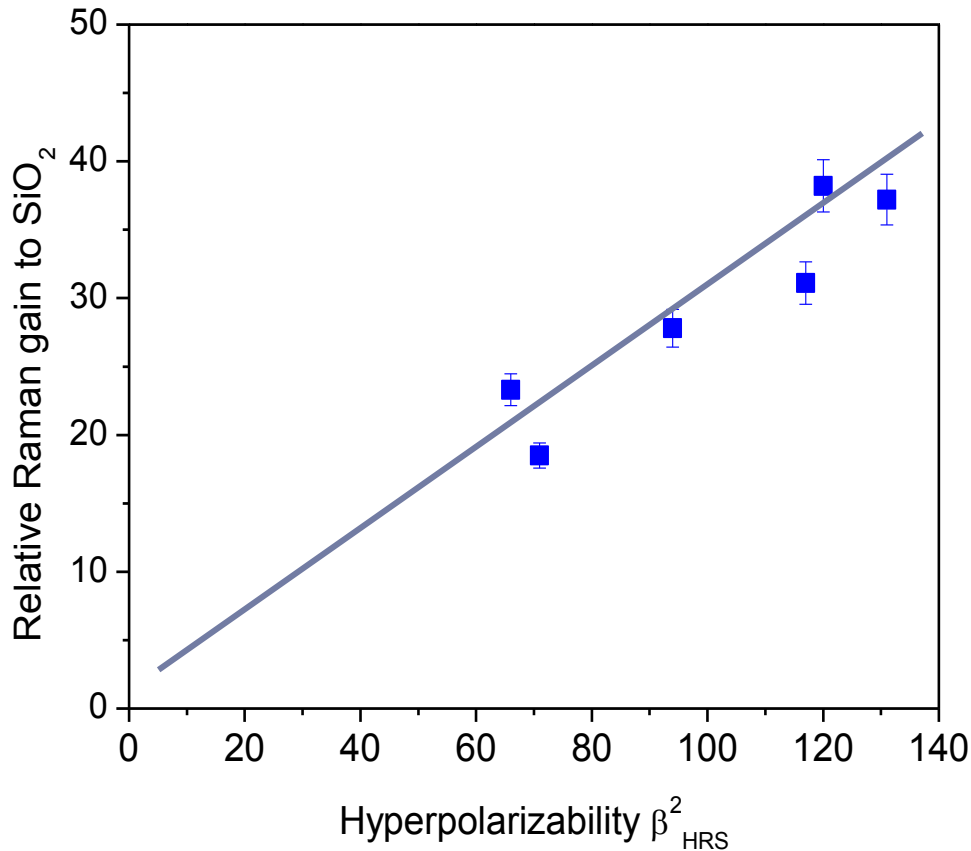
Hyper Rayleigh



→ Reduction of the **tellurite network polarization**.

Drastic decrease of the hyperpolarizability during the ZnO introduction.

Hyperpolarizability and Raman Gain

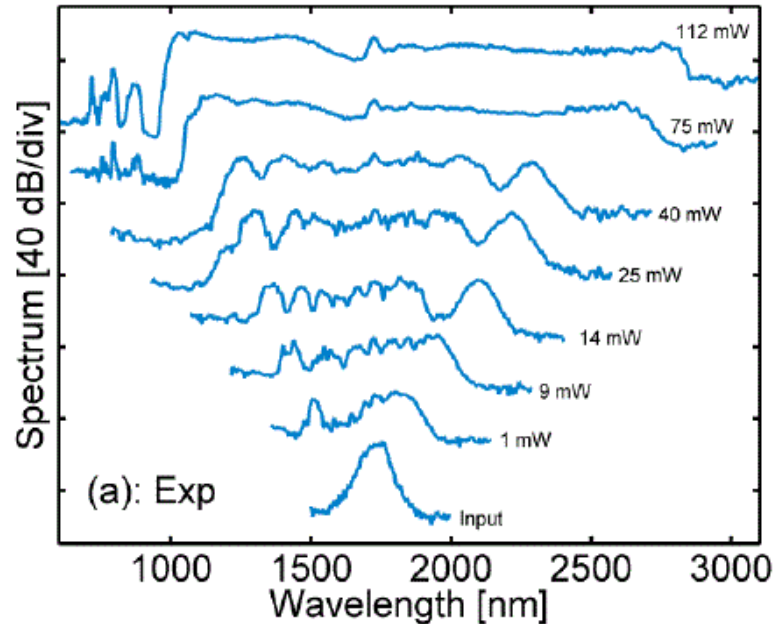


- **Raman gain** linearly proportional to **hyperpolarizability** ($\chi^{(2)} \propto \chi^{(3)}$)

→ Relationship between a **local measurement** (*hyperpolarizability*) and a **macroscopic property** (*Raman gain*)

Supercontinuum generation

80TeO₂-10ZnO-10Na₂O



I. Savelii et al., Optics Express, Vol. 20 Issue 24, pp.27083-27093 (2012)

Self phase modulation

Raman Gain

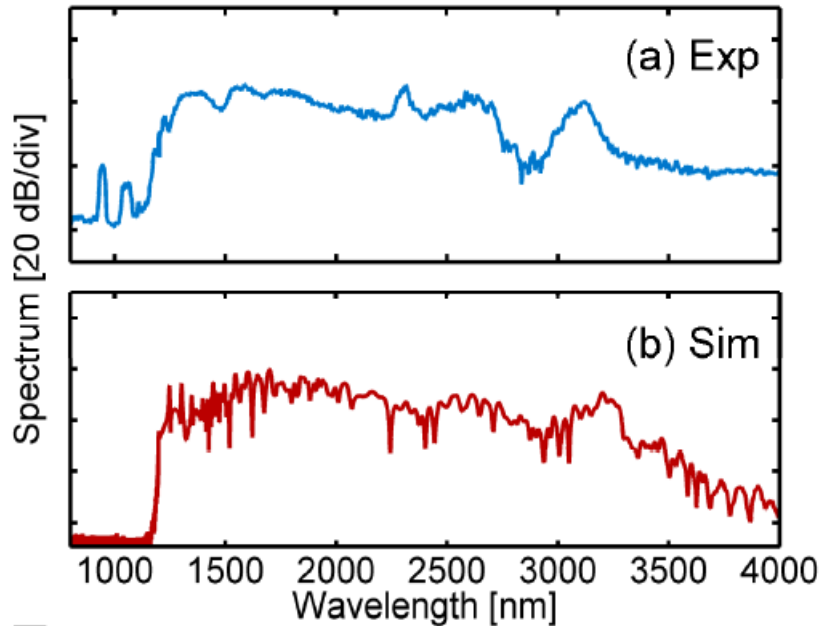
Four Wave Mixing

THG

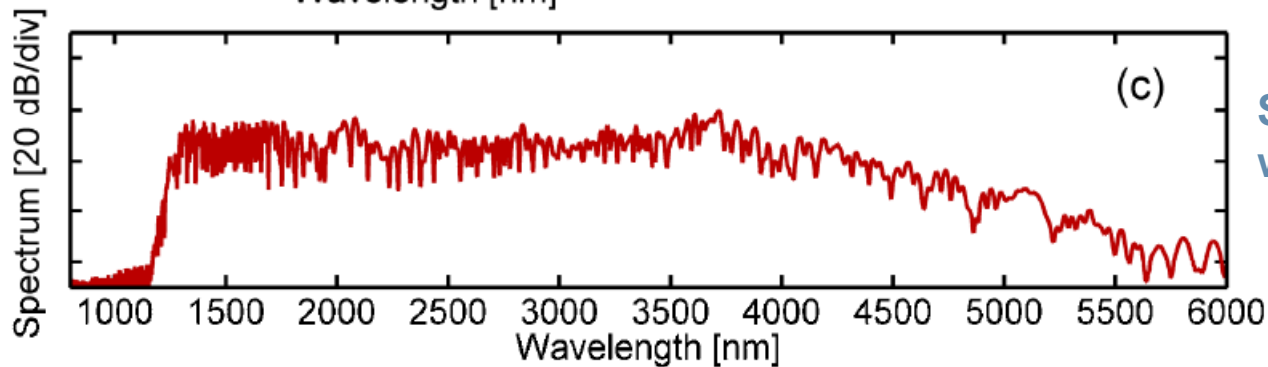
Theoretically up to 3000 nm if no Hydroxyls

M. Liao, Optics Express, 20, 26 (2012), p574

Supercontinuum generation

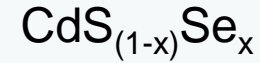
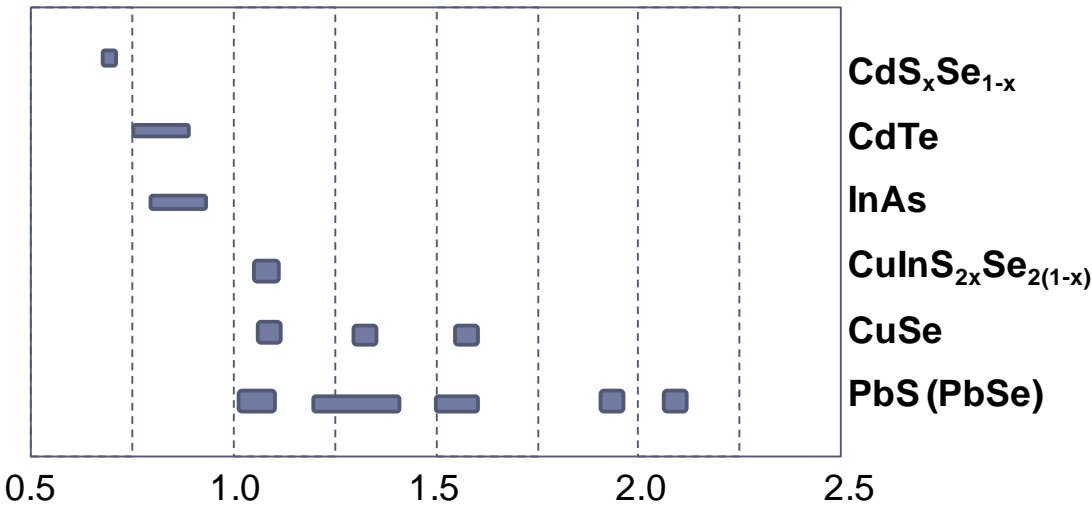


*I. Savellii et al., Optics Express,
Vol. 20 Issue 24, pp.27083-27093 (2012)*



**Simulation
without SH and OH groups**

Quantum dots for NLO



$$W = \Delta n_{\text{sat}} / \alpha_0 \tau$$

*Finlayson et al.,
Vol. 6, No. 4/April 1989/J. Opt. Soc. Am. B*

Glasses doped semiconductor quantum dots

PbS , PbSe , PbTe

- narrow band-gap,
- large optical nonlinearity
- fast response time

*S. Ju,
Optics Express, 19, 3, (2011), p2599*

metallic nanoparticles for NLO

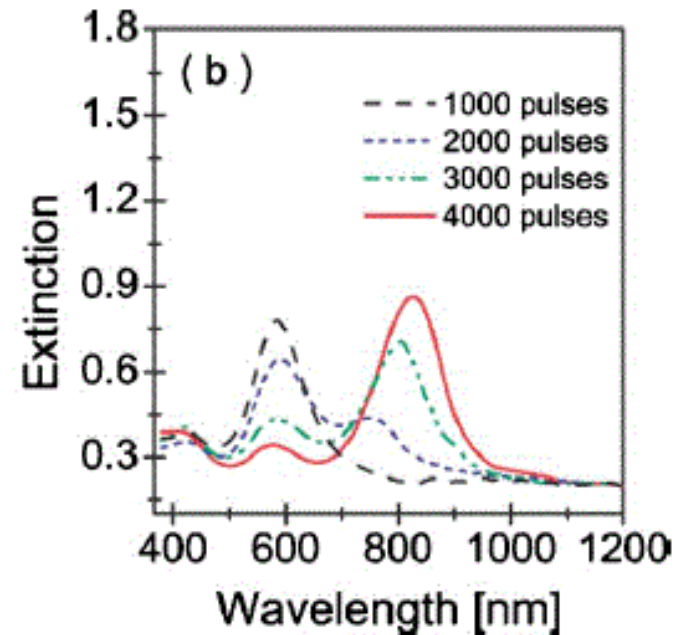
non-spherical
silver nanoparticles



**Enhancement of nonlinearity
2 order of magnitude**

A. Stalmashonak ,
Optics Letters 35, 10, (2010), p1673
S. Mohan
Optics Express, 20, 27, (2012, p28655

Large aspect ratio
metal nanoparticles



Second order nonlinearity

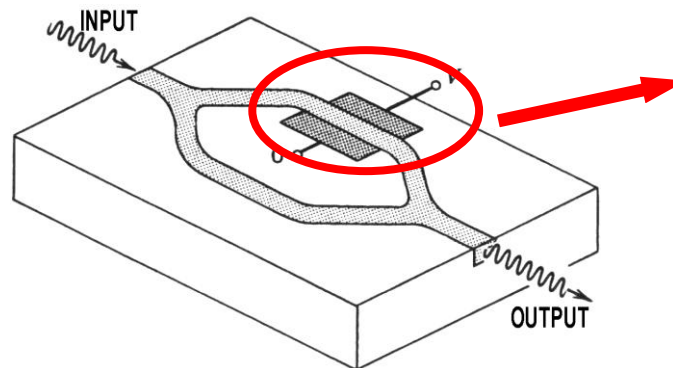
□ Nonlinear optical effects

$$\mathbf{P} = \varepsilon_0 (\chi^{(1)}\mathbf{E}(\omega) + \chi^{(2)}\mathbf{E}(\omega)\mathbf{E}(\omega) + \chi^{(3)}\mathbf{E}(\omega)\mathbf{E}(\omega)\mathbf{E}(\omega) + \dots)$$

SHG (2ω)
 $n \approx f(E)$

$$n = n_0 + \zeta E$$

Applications

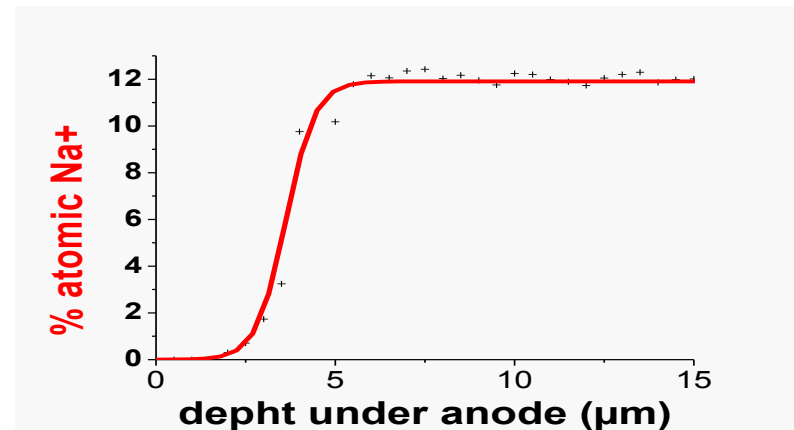
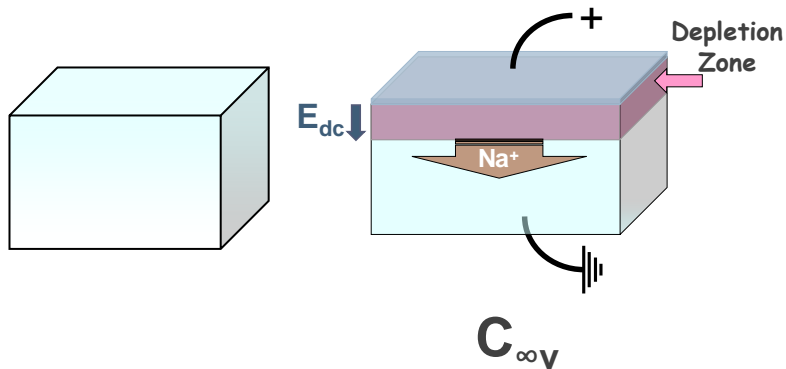
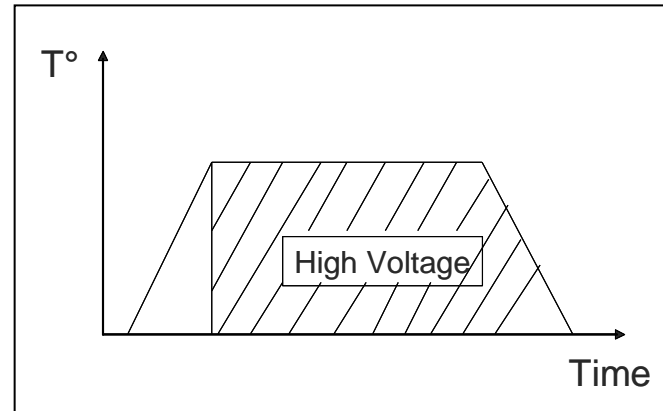
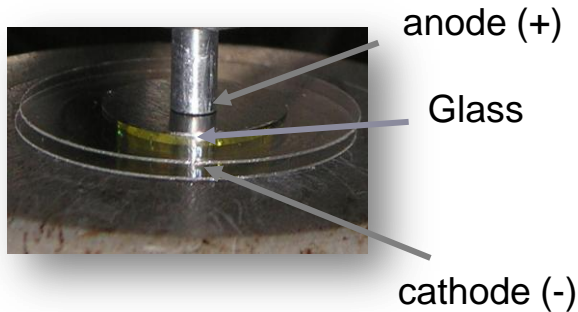


Variation of
the refractive index

Modulation or switching
of the light

Thermal Poling

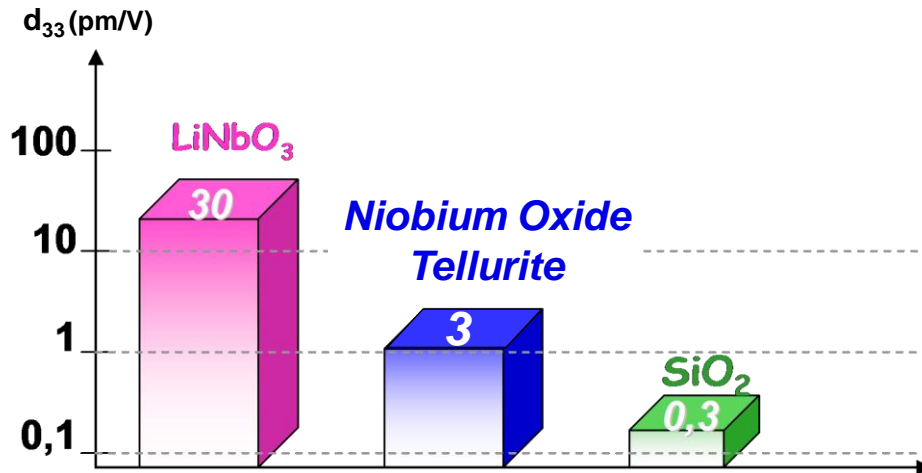
Sample placed between two electrodes



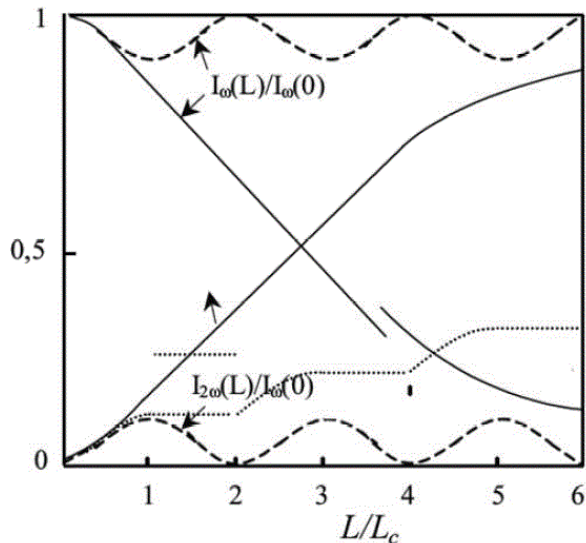
$$\text{PNL}(2\omega) = \chi^{(3)} E_{\text{dc}} E(\omega)E(\omega)$$

$$\approx \chi^{(2)}$$

Material performance



$$P^{NL}(2\omega) = \chi^{(3)} E_{dc} E(\omega)E(\omega) \approx \chi^{(2)}$$



Need for quasi phase matching

P. N. Butcher and D. Cotter, *The elements of non linear optics*. Cambridge University press, 1990.

Structuration of SHG

Ag thin film (200 nm) :

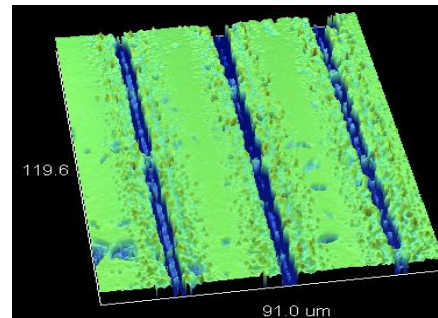
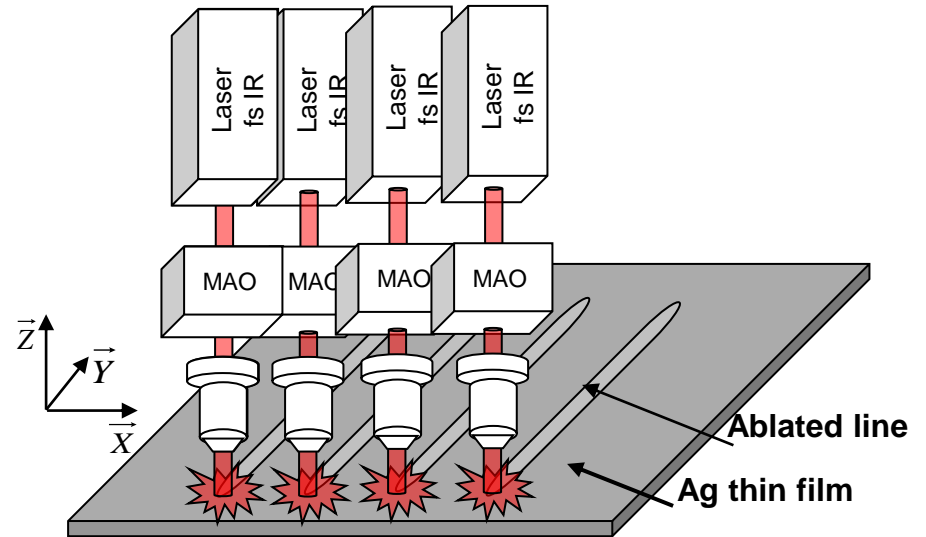
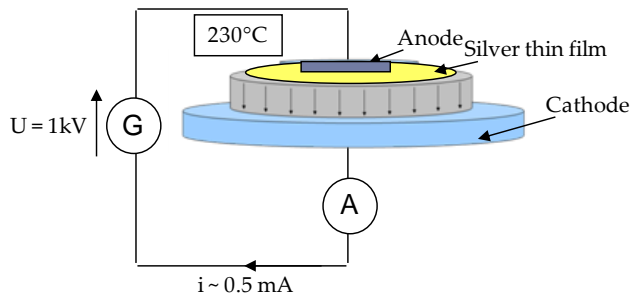
Anode

Laser Ablation of Ag Lines

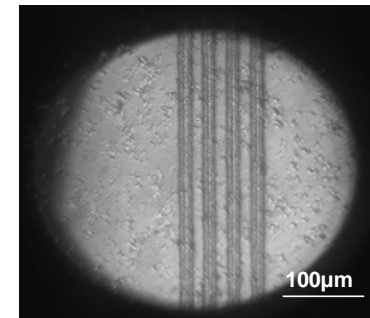
Structured Anode

Thermal poling

230 °C, t = 1 h, U = 1 kV, $i_0 \sim 0.5$ mA

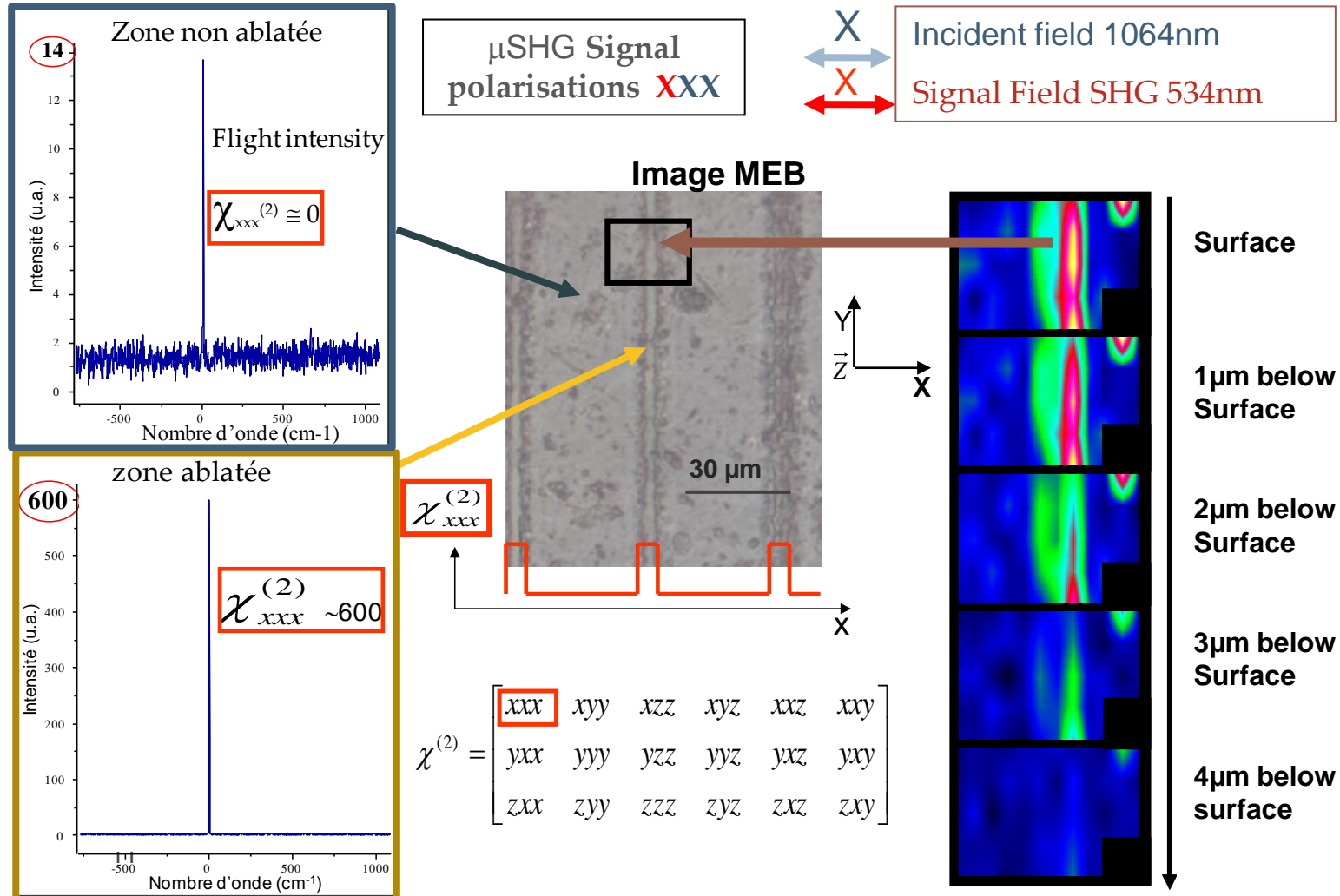


Surface profile after laser ablation



SEM

Analysis of μ SHG signal

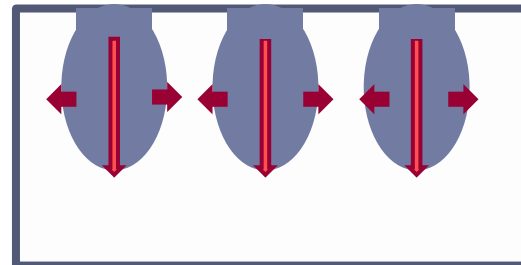
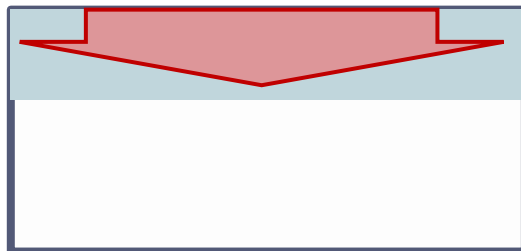


Symmetry control

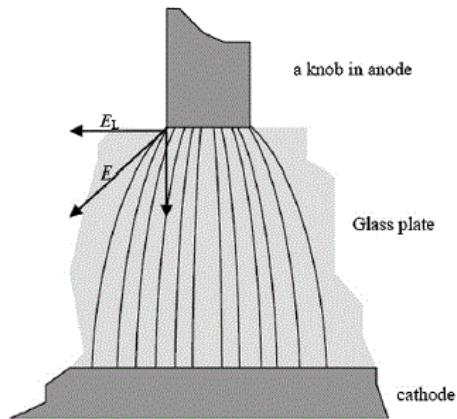
(a) polarisation $C_{\infty v}$ (axe z)

$$\chi^{(2)} = \begin{bmatrix} 0 & 0 & 0 & 0 & xxz & 0 \\ 0 & 0 & 0 & xxz & 0 & 0 \\ zxx & zxx & zzz & 0 & 0 & 0 \end{bmatrix}$$

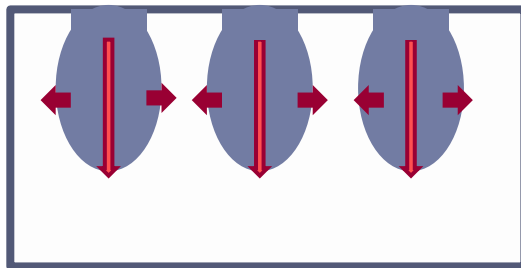
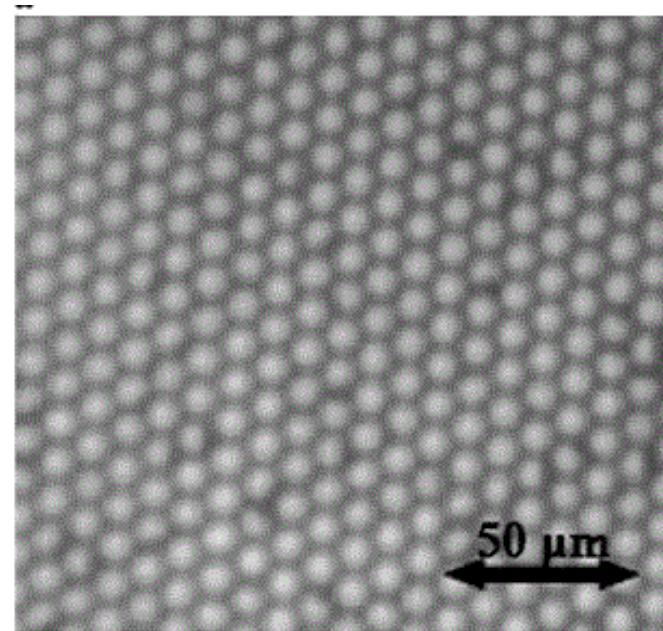
(b) ablation + polarisation C_s (plan xz)

$$\chi^{(2)} = \begin{bmatrix} xxx & xyy & xzz & 0 & xxz & 0 \\ 0 & 0 & 0 & yyz & 0 & yyx \\ zxx & zyy & zzz & 0 & zzx & 0 \end{bmatrix}$$


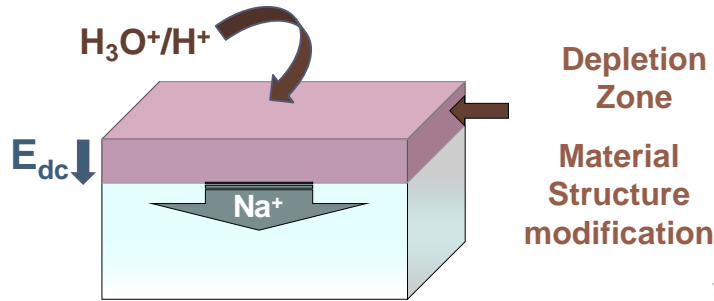
Pattern implementation



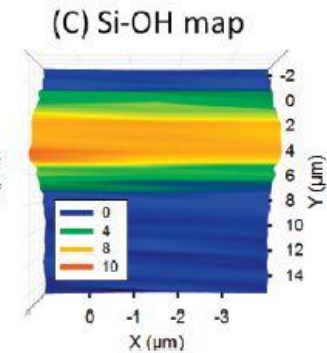
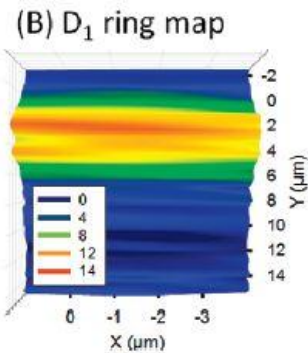
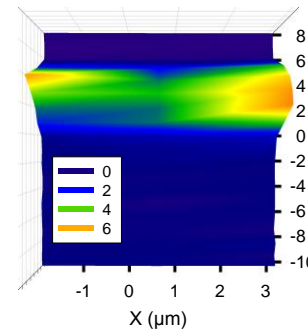
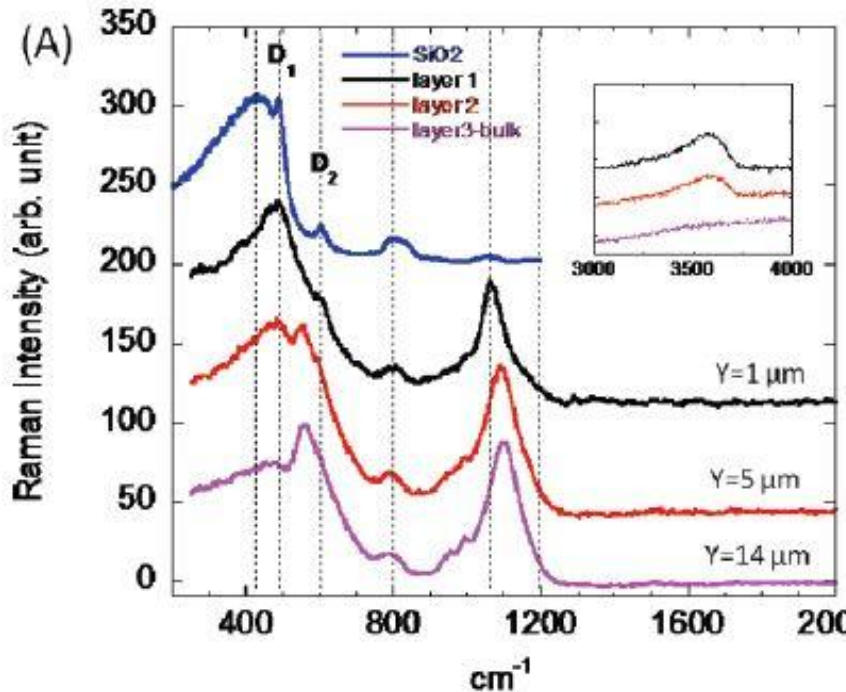
- A. Lipovskii et al.,
- B. *Solid State Ionics* 181 (2010) 849–855



Materials structure modification

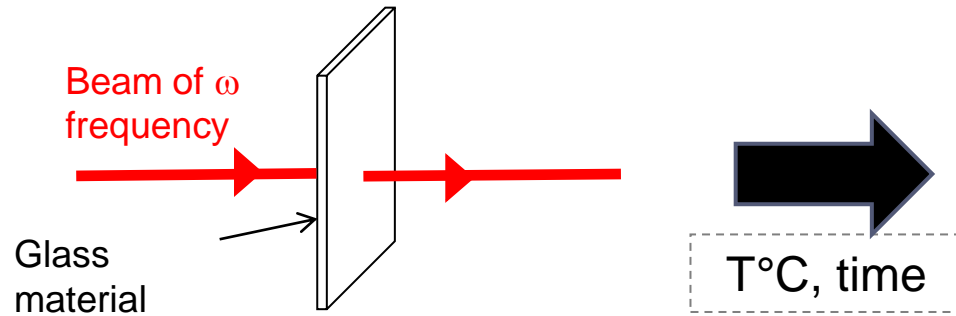


Silicate

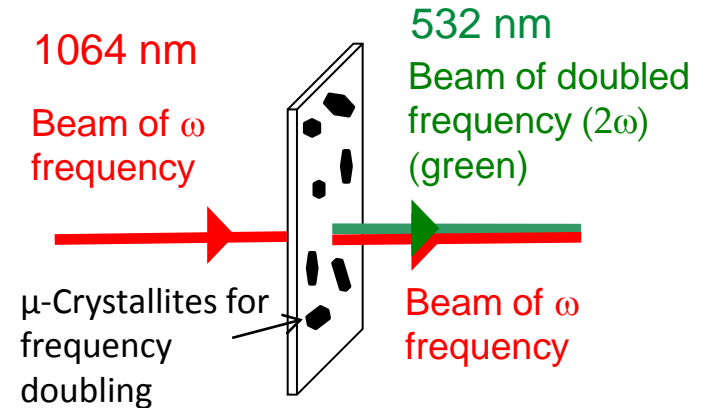


M. Dussauze et al., *The journal of physical chemistry. C*
 Vol. :114 iss :29 ,2010, 12754 -12759.

A glass-ceramic for frequency doubling



Before heat treatment
Centrosymmetric glass



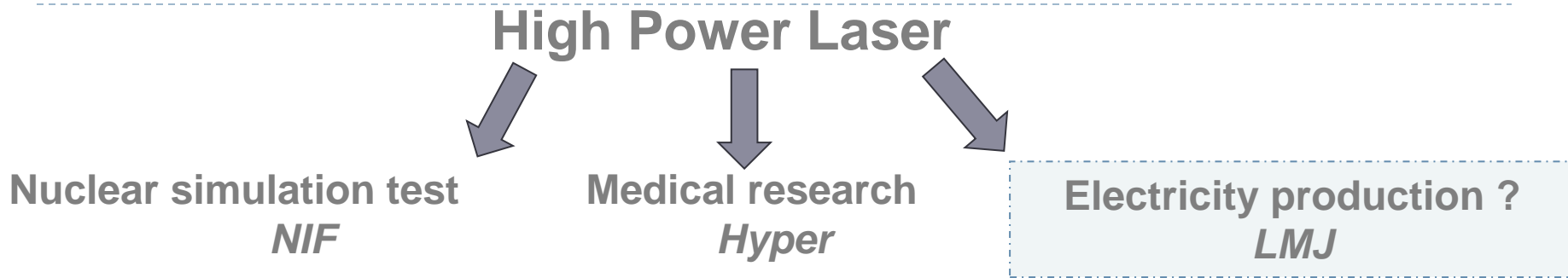
After heat treatment
Non-Centrosymmetric crystallites

➤ Characteristics :

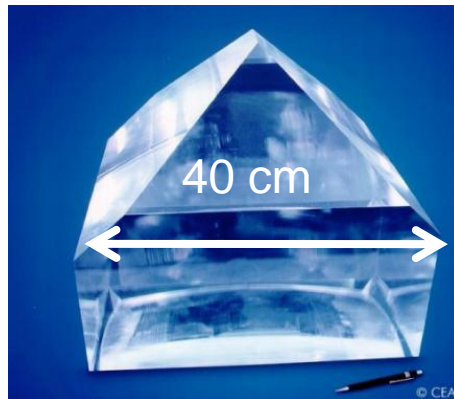
Size and space control of μ -crystallites precipitation :

- Sub – micro or nano crystals for **transparency** or **low refractive index difference** between the **matrix** and the **crystallites**
- Homogenous **bulk crystallization**

H. Jain,
Ferroelectrics, 306, 111-127 (2004)



Current material :



- Large-sized Monocrystals
- Cut out with a specific way

} ↗ Cost

Potassium Dihydrogen Phosphate

Vitroc ceramic for NLO

KNbO_3
 KTiOPO_4 (KTP)
 $\text{Ba}_2\text{TiSi}_2\text{O}_8$
 LiNbO_3

SHG Increases
with crystallization ratio

Trade off to be reached:

Transparency/SHG activity

Control of low refractive index difference between the crystalline phase and the glass

$25\text{La}_2\text{O}_3$ - $25\text{B}_2\text{O}_3$ - 50GeO_2
Crystalline phase LaBGeO_5
(200 nm à 200 μm)

$15\text{K}_2\text{O}$ - $15\text{Nb}_2\text{O}_5$ - 68TeO_2 - 2MoO_3
Crystalline phase KNbO_3

Effect of Poling

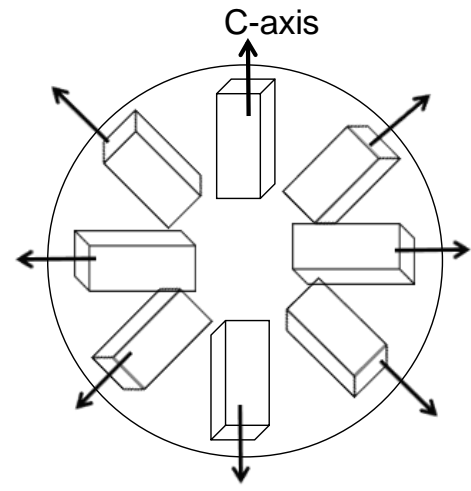
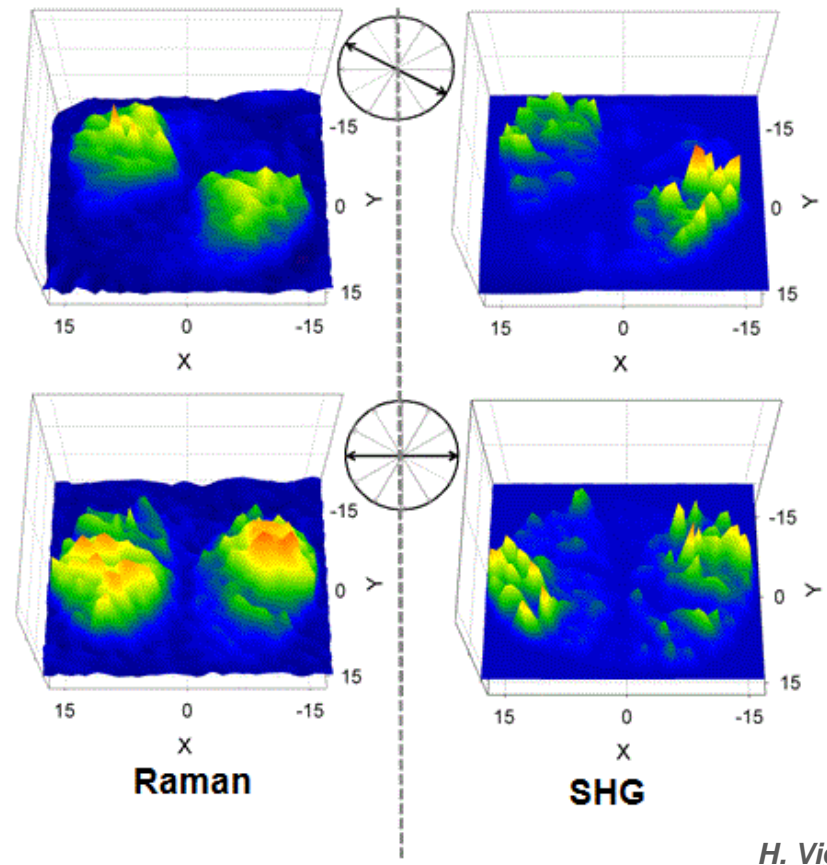
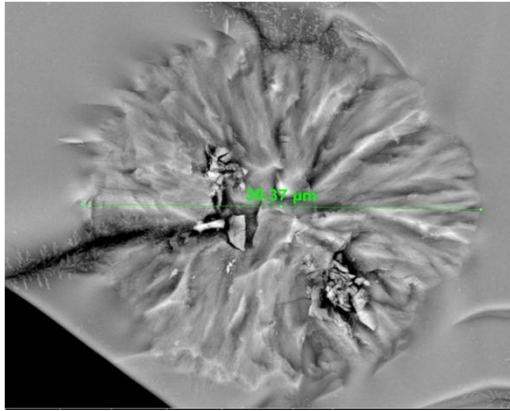
$15\text{K}_2\text{O}$ - $15\text{Nb}_2\text{O}_5$ - 68TeO_2 - 2MoO_3 , Crystallites KNbO_3
Second order NLO increase by a factor 6 to 20 [58].

In $0.7\text{Na}_2\text{B}_4\text{O}_7$ - $0.3\text{Nb}_2\text{O}_5$, Crystallites NaNbO_3 (30 nm)
SHG signal measured after poling

Spherulite



X, Y axis : 30 X 30 μm



Radial distribution

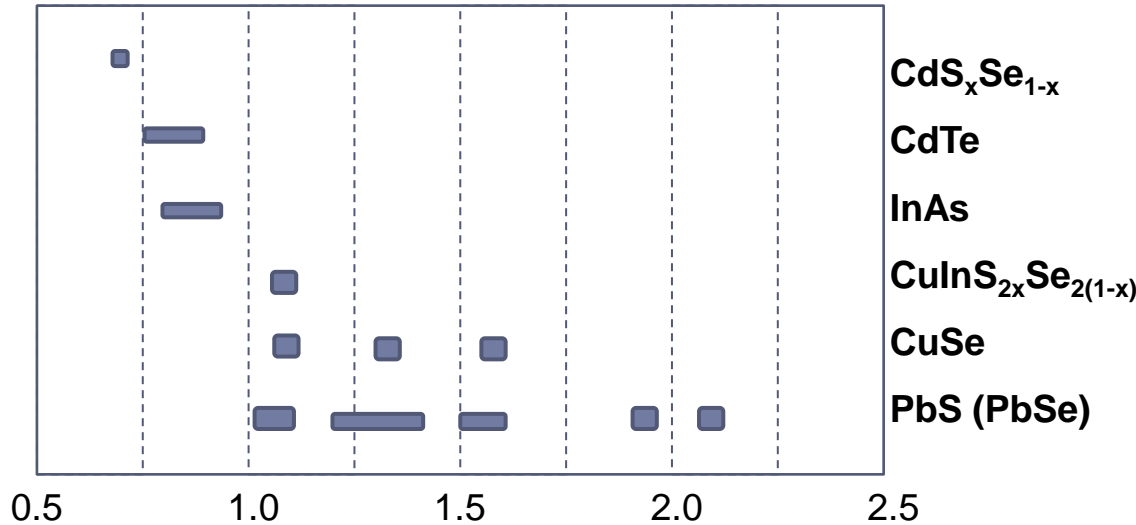
Spherulites distributed in the matrix with distances greater than the coherence length,
Total second harmonic intensity
Sum of the individual contributions (incoherent case).

Similar phenomenon in $25\text{La}_2\text{O}_3\text{-}25\text{B}_2\text{O}_3\text{-}50\text{GeO}_2$
Cristalline phase LaBGeO_5

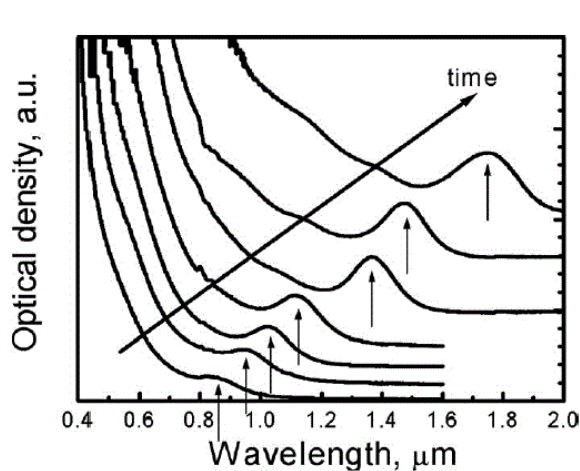
H. Vigouroux
Adv. Funct. Mater. 2012, 22, 3985–3993

Nonlinear absorption

*A.M. Malyarevich, et al.,
J. Appl. Phys. 103, 081301 2008*



Q switching and mode locking of near-infrared solid-state lasers to obtain light pulses of high power and short/ultrashort duration



PbSe

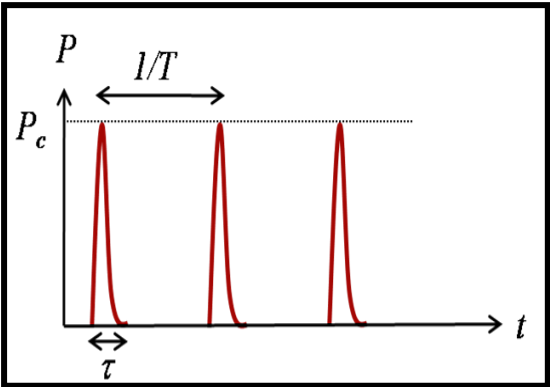
Key parameters :

Ground-state absorption cross section,
Residual non saturable absorption,
Bleaching relaxation absorption recovery time (ps)
Saturation intensity

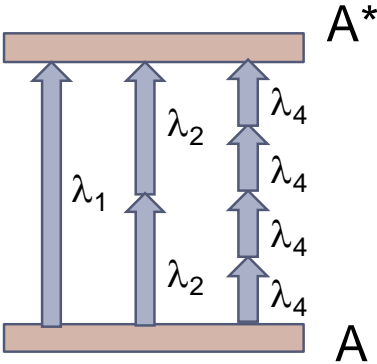
Size distribution : 5%–10% around their main diameter

Nonlinear absorption

Short pulsed Lasers



$P_c \approx \text{GW} - \text{TW}$



Nonlinear effect
= multiphoton

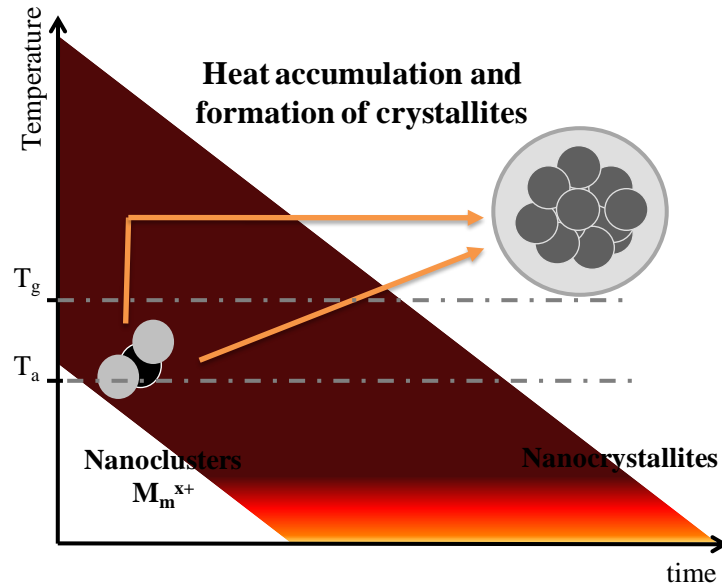
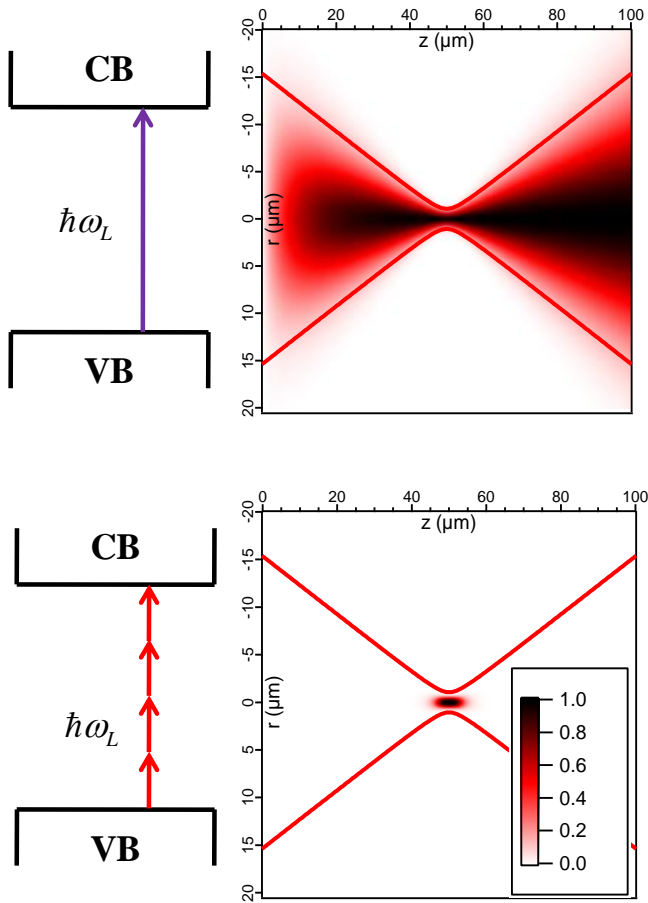
Localized absorption



Dye Fluorescence in solution

Linear effect:
Absorption along the light propagation

Nonlinear Absorption

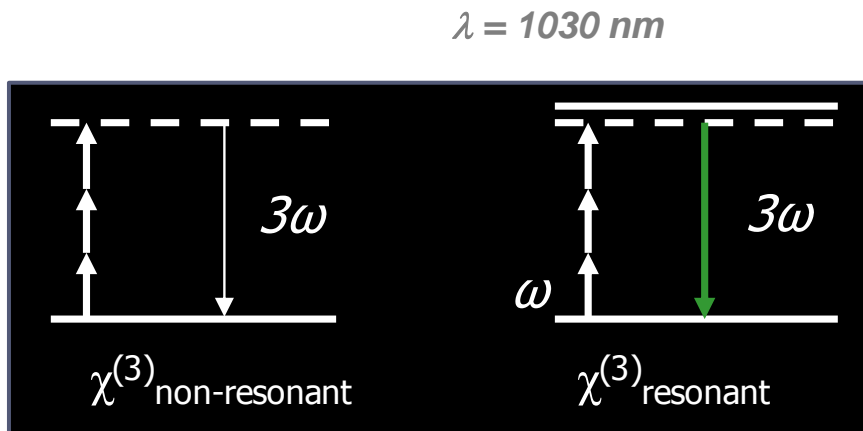


Possible to implement
local $\chi^{(2)}$ and $\chi^{(3)}$

Local THG in silver containing glass

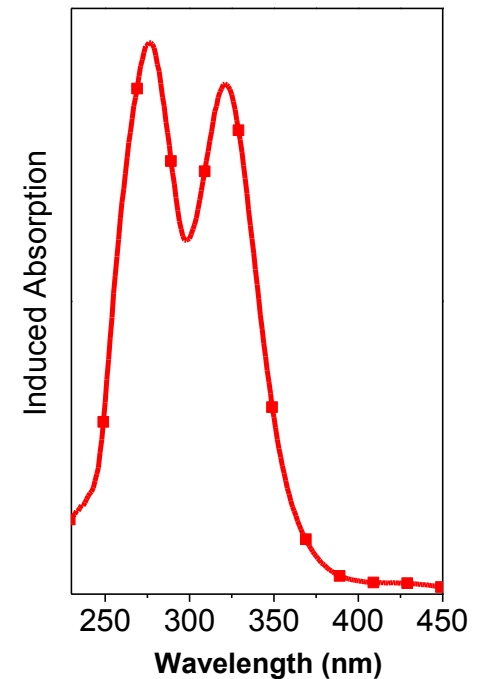
THG microscopy

3ω resonant species induced by femtosecond laser irradiation

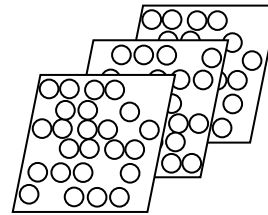
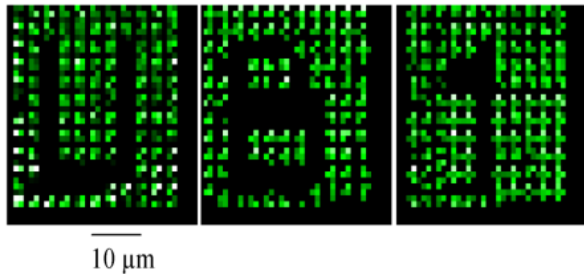


Local Formation of Clusters

Ag_m^{x+}
(formed of Ag^0 atoms and Ag^+ ions)



THG for data storage



*L. Canioni, Optics Letters,
Vol. 33 Issue 4, pp.360-362 (2008)*

**Exaltation of
the THG signal
due to the resonance**

3D data recording and reading

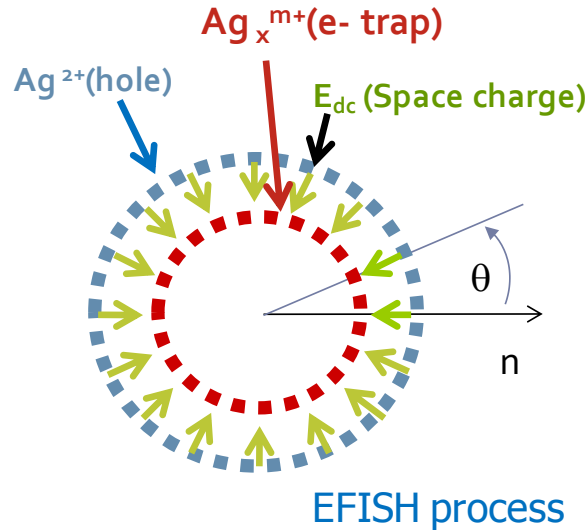
Nonlinear optical process



Confocal per nature

Local SHG in silver containing glass

Silver containing phosphate glass



Laser:

Wavelength: 1.04 μm

Duration: 400 fs

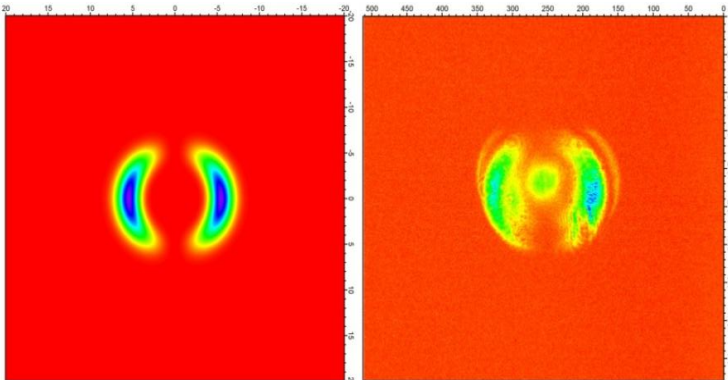
Repetition rate: 10 Mhz

$$\text{PNL}(2\omega) = \chi^{(3)} E_{dc} E(\omega)E(\omega) \approx \chi^{(2)}$$

EFISH process

Theoretical SHG

Measured (HH) SHG



Charge separation process

And thanks to the glass composition

Stabilization of the charge separation

- Understanding of the relation **glass structure / NLO properties**
 - ✓ resonant (**Raman gain, Nonlinear absorption**)
 - ✓ non-resonant (**Kerr effect, THG**)
 - ✓ **Nonlinear absorption**
- Impact of **glassceramics** (Loss issues)
 - ✓ **Second order nonlinearity**
 - ✓ **Metal** or **semiconductor**
- Control of **local phase separation** or **local crystallization**
 - ✓ **Third order** and **Second order nonlinearity**

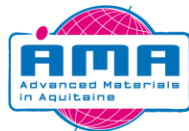
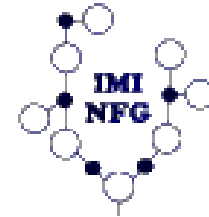
↘ Acknowledgments

P. Thomas, J.R. Duclere
S.P.C.T.S., Université Limoges, France.

J. Trebosc, B. Revel, L. Montagne
UCCS, Université Lille Nord de France, France

L. Petit, K. Richardson
COMSET, Clemson University, USA

J.Y. Choi, C. Rivero, G. Stegeman, M. Richardson
CREOL, University of Central Florida, USA
*(*co-tutelle de thèse-Univ. Bordeaux1)*



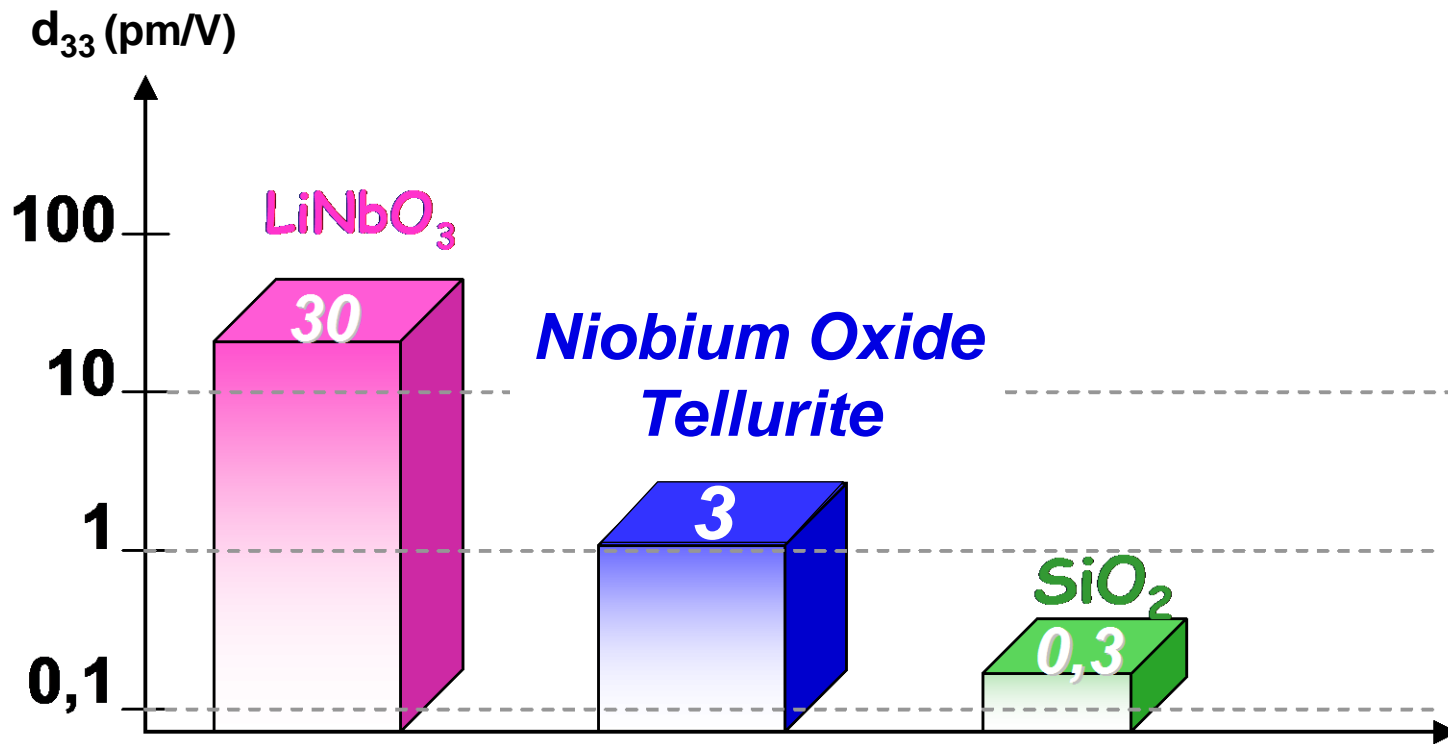
Supercontinuum

Table 1. Various highly nonlinear fibers and their SC generations in picosecond regime. 10 dB bandwidths were obtained from the SC spectra in the publications. When determining the 10 dB bandwidth, the strong pump peak was excluded.

Fiber	Pump wavelength (nm)	Nonlinear coefficient ($\text{km}^{-1}\text{W}^{-1}$)	Fiber length (m)	Pulse width (ps)	Peak power of pulse (W)	SC total bandwidth (nm)	10 dB bandwidth (nm)
Our tapered fiber	1064	800-5500	0.75	15	375	350-2000	780-1890
Silica tapered fiber [20]	1064	8-40	2	3-4	19608-32680	350-1750	380-1750
Silica microstructured fiber [21]	1064	-	2	21	24000	400-2250	420-1620
Silica microstructured fiber [22]	1064.5	8.5	100	600	4200	600-1750	650-1750
Silica microstructured fiber [5]	647.1	150	3	60	400	440-1130	480-940
Silica microstructured fiber [23]	1050	11	5	350	8893	400-1700	600-1700

M. Liao, Optics Express, 20, 26 (2012), p574

Material performance



SHG nanocrystallites

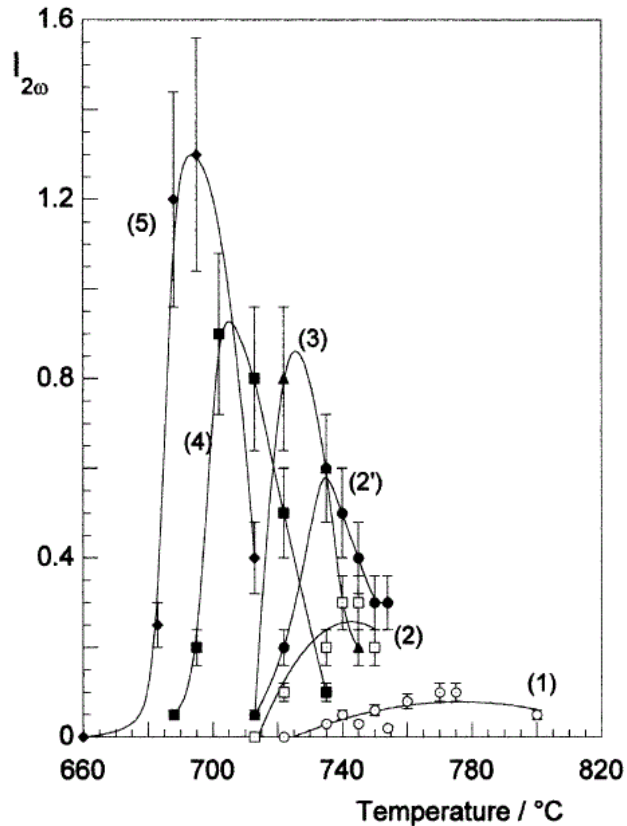
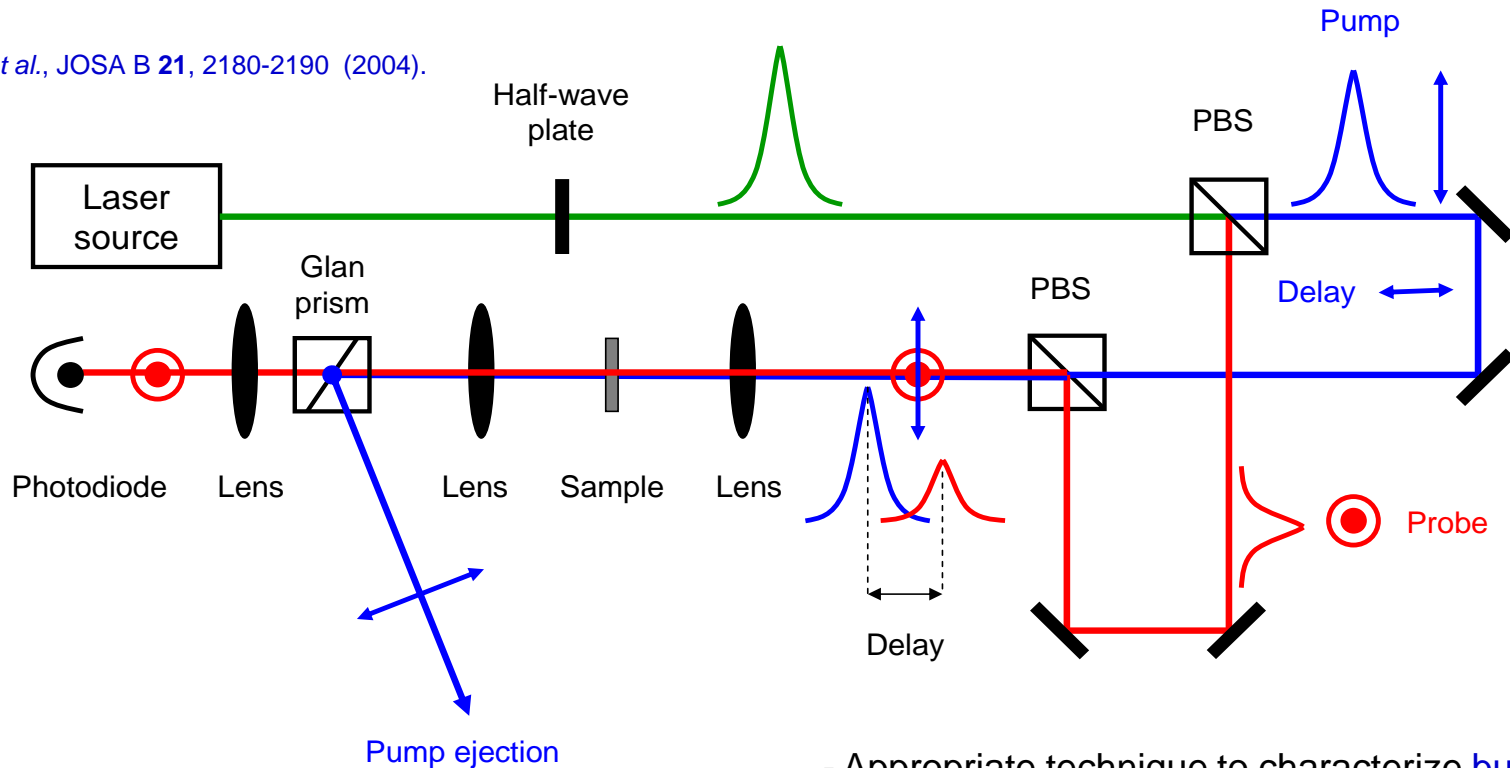


Fig. 4. SHG efficiency of KNS glasses vs heating temperature for 24 h and 48 h (no. 2') treatments.

SHG efficiency can be connected to combination of third-order non-linearity with spatial modulation of linear polarizability

Pump-probe experimental setup

Santran *et al.*, JOSA B **21**, 2180-2190 (2004).



- Absolute measurements.
- Measurement uncertainty ~10%.

- Appropriate technique to characterize **bulk materials**.
- Difficult to implement on **structured materials** (maintain of the polarization under microscope, small nonlinear interaction length, etc...).